Meta-Analysis Reveals Consensus Genomic Regions Associated with Multiple Disease Resistance in Wheat (*Triticum Aestivum L.*)

Dinesh Kumar Saini
Punjab Agricultural University
Amneek Chahal
Agricultural University, Ludhiana
Neeraj Pal
G. B. Pant University of Agriculture and Technology
Puja Srivastava
Punjab Agricultural University
Pushpendra Kumar Gupta (pkgupta36@gmail.com)
Ch. Charan Singh University https://orcid.org/0000-0001-6374-9148

Research Article

Keywords: meta-QTL analysis, wheat, multiple disease resistance, genome-wide association studies, candidate genes

Posted Date: September 29th, 2021

DOI: https://doi.org/10.21203/rs.3.rs-773587/v1

Version of Record: A version of this preprint was published at Molecular Breeding on February 21st, 2022. See the published version at https://doi.org/10.1007/s11032-022-01282-z.

Abstract

In wheat, meta-QTLs (MQTLs), and candidate genes (CGs) were identified for multiple disease resistance (MDR). For this purpose, information was collected from 58 studies for mapping QTLs for resistance to one or more of the five diseases. As many as 493 QTLs were available from these studies, which were distributed in five diseases as follows: septoria tritici blotch (STB) 126 QTLs; septoria nodorum blotch (SNB), 103; fusarium head blight (FHB), 184; karnal bunt (KB), 66, and loose smut (LS), 14. Of these 493 QTLs, only 291 QTLs could be projected onto a consensus genetic map, giving 63 MQTLs. The CI of the MQTLs ranged from 0.04 to 15.31 cM with an average of 3.09 cM per MQTL. This is a ~ 4.39 fold reduction from the CI of initial QTLs, which ranged from 0 to 197.6 cM, with a mean of 13.57 cM. Of 63 MQTLs, 60 were anchored to the reference physical map of wheat (the physical interval of these MQTLs ranged from 0.30 to 726.01 Mb with an average of 74.09 Mb). Thirty-eight (38) of these MQTLs were verified using marker-trait associations (MTAs) derived from genome-wide association studies. As many as 874 CGs were also identified which were further investigated for differential expression using data from five transcriptome studies, resulting in 194 differentially expressed genes (DEGs). Among the DEGs, 85 genes had functions previously reported to be associated with disease resistance. These results should prove useful for fine mapping of MDR genes and marker-assisted breeding.

Introduction

The concept of multiple disease resistance (MDR) is not new. Nene (1988) reviewed the information on MDR in legumes and Pooja et al. (2014) described the phenomenon of MDR in wheat. More recently, Wiesner-Hanks and Nelson (2016) discussed the available evidence related to the MDR in plants. The occurrence of MDR is not surprising, because the high level of correlations has often been observed between resistance against each of several individual diseases, suggesting the occurrence of pleiotropic loci or tightly linked clusters of *R* genes for resistance against several diseases (Wiesner-Hanks and Nelson, 2016). Multi-trait (MT) analysis for quantitative disease resistance involving more than one correlated diseases has also been undertaken, and multi-trait QTLs for disease resistance have been identified, suggesting that there may be complex loci, which control resistance against more than one disease (Hernandez et al., 2012).

Generally, different genes or gene systems are available for resistance against different individual diseases, irrespective of whether we are dealing with race-specific resistance or race non-specific, broad-spectrum, durable resistance or adult plant resistance (APR) (Kou and Wang, 2010). MDR differs from this broad-spectrum resistance or race non-specific durable resistance or APR, which generally means resistance against the majority of prevalent races for a particular disease, and not the resistance against a number of diseases (Wiesner-Hanks and Nelson, 2016). Similarly, APR is often used to provide durable resistance, but this also generally deals with resistance against an individual and specific diseases, one at a time.

QTL analysis has considerably improved our understanding of disease resistance inheritance and underlying genetic architecture. Nonetheless, genes/QTLs providing resistance against multiple diseases are largely unknown. Very few studies are available, where genes or QTLs for resistance to multiple diseases have been discovered (Hernandez et al. 2012; Jighly et al. 2016; Zwart et al. 2010; Mago et al. 2011). In general, to breed for multiple disease resistance (MDR), the pyramiding of multiple QTLs/genes for different diseases has been conducted by wheat breeders (Gupta et al. 2021a; Sharma et al. 2021; Rana et al. 2021). However, this method is a lengthy process as it starts with combining two QTLs for two different diseases into one line, and then, as the generation is established, another QTL is integrated to achieve the desirable phenotype. In addition, the QTLs for individual diseases that are introgressed might have epistatic interaction, which may alter the outcome of the introgression process.

STB, SNB, FHB, KB, and LS are important wheat diseases, worldwide. Each of these diseases can cause 10–15% yield losses, which can sometimes approach 50% in favourable weather conditions, especially in low-input agriculture, where disease control is generally poor (Duveiller et al. 2007). Aiming to understand the genetic basis of resistance to these five diseases, numerous QTL studies involving different populations have also been carried out in recent years which resulted in the identification of hundreds of resistance QTLs for each disease (Online S1, S2). The idea of MDR also prompted the development of MQTLs using QTLs for each of several individual diseases. Meta-QTL analysis for identification of MQTLs for MDR have already been conducted in barley (Schweizer and Stein, 2011), maize (Ali et al., 2013), and rice (Kumar and Nadarajah 2020). However, no meta-QTL analysis has been conducted so far for multiple disease resistance (MDR) in wheat.

In the present study in wheat, meta-QTL analysis was used for the identification of MQTLs for MDR involving five different diseases, namely STB, SNB, FHB, KB, and LS; for this purpose, already published mapping studies about these five diseases were used. Since QTLs associated with FHB reported up to the year 2019 have regularly been utilized for the identification of MQTLs (Liu et al. 2009; Löffler et al. 2009; Cai et al. 2019; Venske et al. 2019; Zheng et al. 2020); QTL studies published after the year 2019 were only included in the present analysis. Further, results of the meta-analysis were integrated with genome-wide association studies (GWAS), and transcriptomics to identify the promising genomic regions and important CGs, which affect MDR in wheat. This work may help to lay a foundation for the identification, transfer, and aggregation of the identified promising MQTLs or CGs in wheat breeding for multiple disease resistance.

Materials And Methods

Bibliographic survey and collection of data on QTLs

Using PubMed (https://pubmed.ncbi.nlm.nih.gov/) and Google Scholar (https://scholar.google.com/), an extensive search for publications reporting QTLs associated with STB, SNB, FHB, KB and LS resistances in wheat was performed. The following information was collected and compiled from each mapping study: type and size of the population, flanking markers and their genetic positions on the map, peak

position of the QTLs, PVE values, and LOD scores of the individual QTLs. Wherever there was no information available on the peak position, the mid-position of the two flanking markers was taken as the peak. Similarly, when the LOD score of an individual QTL was not available, a LOD score of 3.0 was used. For the QTLs, lacking original confidence interval (CI), CI (95%) was calculated based on population-specific equations derived from different simulations (Darvasi and Soller, 1997; Guo et al. 2006). Studies lacking necessary information required for analysis such as PVE values and genetic positions of markers were excluded from the analysis (e.g., Knox et al. 2014; Simón et al. 2004).

Construction Of The Consensus Map

A consensus genetic map including AFLP, SSR, RFLP, DArT, KASP, RAPD, SNP, and some gene-specific markers was constructed using LPmerge software (Endelman and Plomion 2014). For this purpose, the following five high-quality genetic maps were utilized: the 'Wheat, Consensus SSR, 2004' involving 1235 markers (Somer et al. 2004); 'Wheat_Composite_2004' map with 4403 markers, available at GrainGenes database (http://wheat.pw.usda.gov); an integrated durum wheat map with 3669 markers (Marone et al. 2013); and two SNP maps assayed by the platforms Illumina 9K iSelect Beadchip Assay (Cavanagh et al. 2013) and Illumina iSelect 90K SNP Assay (Wang et al. 2014). Further, markers flanking the initial QTLs reported in individual studies were also included on the consensus genetic map.

Qtl Projection And Meta-qtl Analysis

Following the approach described by Chardon et al. (2004), available QTLs were projected onto the newly generated consensus map using the projection tool (QTLProj) available in Biomercator v4.2 software. Meta-QTL analysis was then performed using the same software Biomercator v4.2 (Arcade et al. 2004; Sosnowski et al. 2012). For analysis, two distinct approaches were used, depending on the number of QTLs available for each chromosome. If the number of QTLs on an individual chromosome was ≤ 10, the approach proposed by Goffinet and Gerber was used; if the number of QTLs on an individual chromosome was > 10, the second approach proposed by Veyrieras et al. (2007) was utilized. The model with the lowest Akaike Information Criterion (AIC) value was chosen as the best fit in the first approach. In the second approach, the best model was chosen among the AIC, corrected Akaike Information Criterion (AICc and AIC3), Bayesian Information Criterion (BIC), and Average Weight of Evidence (AWE) models. The model with the lowest criteria in at least three of the models was chosen as the best fit model.

The MQTLs were named based on their genetic positions; for instance, MQTLs mapped on chromosome 1A were named as MQTL1A.1, MQTL1A.2, and so on. The PVE value and LOD score of an MQTL were calculated as the mean of PVE values and LOD scores of initial QTLs contained in the MQTL. The sequences of flanking markers (retrieved from databases, such as GrainGenes, and CerealDB, etc.,) of each MQTL were BLASTed against the Chinese spring reference genome available at Ensembl Plants database (https://wheat.pw.usda.gov/blast/) to determine their physical coordinates. Physical positions

of GBS-SNPs were directly searched at JBrowse wheat genome browser (https://wheat-urgi.versailles.inra.fr/Tools/Jbrowse).

Comparison of MQTLs with MTAs identified in previous GWAS studies

MQTLs identified in the present study were validated using results of recently published GWA studies. For this purpose, the data from 16 GWA studies involving the five different diseases, published during 2017–2021 were collected. The details of these GWA studies are summarized in Table 1. The phenotypic data used in these studies were collected from 15 different countries, with the population size ranging from 96 to 406, including one durum wheat population, two spring wheat populations, eight winter wheat populations, and five mixed wheat populations of spring and winter wheat. Physical positions of markers (significantly associated with the trait) were obtained either from databases or through BLAST searches. Keeping in view the relatively long linkage disequilibrium (LD) decay distance of wheat (approx. 5Mb), the MTAs detected from GWAS within 5 Mb genomic regions near an MQTL were considered to be co-located (Yang et al. 2021).

Table 1
GWA studies on different wheat diseases (used for comparing MQTLs identified in the present study)

Type of wheat (Panel size)	Marker type/ Number	#MTAs	Environment	References
Winter wheat accessions (mainly cultivars and advanced breeding lines) (96)	DArT/874	38	Argentina	Gerard et al. (2017)
Ethiopian durum wheat landraces and 25 Ethiopian durum improved varieties (318)	SNPs (90 K SNP array)/16223	5	Ethiopia	Kidane et al. (2017)
European winter wheat varieties (371)	SNPs (35 K and 90 K SNP array)/28222	39	Germany	Muqaddasi et al. (2018)
Winter wheat landraces and historical cultivars (175)	SNPs (20K SNP array)/7401	12	Denmark, Estonia, Lithuania, and Sweden	Alemu et al. (2021)
Swiss wheat landraces, breeder's lines and cultivars (188)	SNPs (15 K SNP array)/9284	1	Netherlands	Dutta et al. (2021)
Iranian improved lines, diverse lines and differential lines (185)	SNPs and SilicoDArT/21773	37	Iran	Mahboubi et al. (2021)
Russian historic wheat accessions (295)	DArT and SNPs (12886)	24	Australia	Phan et al. (2018)
Hard winter wheat association mapping panel (274)	SNPs (90 K SNP array)/15590	7	USA	AlTameemi et al. (2021)
Australian breeding lines and accession from CIMMYT wheat germplasm (144)	SNPs (90 K SNP array)/1628	8	India, Mexico	Emebiri et al. (2019)
Landraces, elite lines, released varieties and advanced breeding lines (339)	DArTseq/13098	18	Mexico	Gupta et al. (2019)
Pre-breeding lines (179)	DArTseq SNPs/6382	15	Mexico	Singh et al. (2020)
Soft red winter wheat (360)	GBS-SNPs/71428	10	Arkansas	Holder (2018)
Elite soft red winter wheat cultivars and breeding lines (238)	SNPs (90 K SNP array)/3919	29	USA	Tessmann and Sanford, (2018)

#No. of significant MTAs detected

Type of wheat (Panel size)	Marker type/ Number	#MTAs	Environment	References
Winter wheat cultivars (171)	SNPs (90 K SNP array)/23556	26	China	Hu et al. (2020)
Soft red winter wheat (354)	GBS-SNPs/72634	42	USA	Larkin et al. (2020)
Chinese wheat accessions (406)	SNPs (90 K and 660 SNP arrays)/437343	21	China	Shi et al. (2021)

#No. of significant MTAs detected

Association Of Known Resistance Genes With Mqtls

Information was also collected for the resistance genes associated with the STB, SNB, FHB, KB, and LS diseases to see if they are co-located with the MQTLs identified in the present study. For this purpose, the nucleotide sequences of the markers linked to resistance genes or the gene sequences were BLASTed against the wheat reference genome sequence available in the Ensembl Plants database (https://plants.ensembl.org) and genomic coordinates of the markers or genes were obtained. These physical intervals were then compared with the physical coordinates of the MQTL regions; any resistance gene that fell within a given MQTL region was considered as the MQTL region co-located with the corresponding resistance gene.

Candidate Gene Mining Within The Mqtls

The CGs within the defined physical intervals of promising MQTLs were identified using the BioMart tool (https://plants.ensembl.org/biomart/martview) of Ensembl Plants. MQTLs with a physical interval of less than 2 Mb were directly considered for detection of available CGs; in the remaining cases, when the physical interval was > 2 Mb, the physical position of the MQTL peak was estimated first, and then the complete 2 Mb region surrounding the peak (1 Mb each left and right of the MQTL peak) was investigated to identify the available CGs. Steps followed to estimate the physical intervals of MQTL peaks are available elsewhere (Jan et al. 2021). The function descriptions of identified gene models were extracted from the InterPro database (https://www.ebi.ac.uk/interpro/).

Gene ontology (GO) analysis and expression analysis of the candidate genes

For the CGs detected within the MQTL regions, GO analysis was conducted using the BioMart tool available in Ensembl Plants (https://plants.ensembl.org/index.html). Further, *in silico* expression analysis of CGs was conducted using an expression visualization and integration platform, expVIP (http://www.wheat-expression.com/) (Ramírez-González et al. 2018). For this purpose, five different

expression datasets including expression data related to two diseases, FHB, and ST were utilized based on experiments reported at ExpVIP (Yang et al. 2013; Kugler et al. 2013; Schweiger et al. 2016; Buhrow et al. 2016; Gou et al. 2016).

Following is a summary of these five expression datasets: The first data-set (Yang et al. 2013) consists of differential expression data of a susceptible wheat cv. Sevin, inoculated with *S. tritici* isolate IPO323, with samples collected every day from 3 to 14 days post-inoculation. The second data-set (Kugler et al. 2013) consists of differential expression data of four NILs that carry either of the FHB resistance QTLs, *Fhb1* (NIL2) or *Qfhs.ifa-5A* (NIL3), both of these QTLs (NIL1) or none of them (NIL4, susceptible) in the background of the *FHB* susceptible German spring wheat cv. Remus, treated with *F. graminearum* spore suspension or mock (control), with samples (spike tissues) collected 30 and 50 hours after inoculation. The third data-set (Schweiger et al. 2016) consists of transcriptomic data of two NILs, one NIL carried either *Fhb1* or *Qfhs.ifa-5A* (CM-NIL38) from donor CM-82036 and other (CM-NIL51) carried susceptible alleles from the German spring wheat cv. Remus, treated with *F. graminearum* or mock (control), with head tissues sampled in a dense time-course series from three to 48 h after inoculation. The fourth data set (Buhrow et al. 2016) consists of differential expression data of wheat cv. Fielder challenged with *F. graminearum* GZ3639 spores in the absence and presence of 1.0mM ABA or GA, with spikelets collected 24 hours after inoculation. The fifth data-set (Gou et al. 2016) consists of transcriptomic data of Chinese Spring (moderately FHB-susceptible variety) and CS-7EL (FHB-resistant ditelocentric addition line that contains the long arm of chromosome 7E from *Th. elongatum*) treated with *F. graminearum*, DAOM 180378 or mock, with samples (the inoculated portion of each head) collected 4 days after inoculation.

Transcriptomic data repositories for the remaining three diseases viz., SNB, KB, and LS were not available on ExpVIP. The expression data was obtained in the form of $\log_2$ transformed TPM (transcripts per million) values. Only genes that showed fold change (FC) ≥ 2 or FC ≤ -2, when TPM values were compared under pathogen inoculation versus mock (control), were considered differentially expressed. Further, to analyze the expression patterns of the differentially expressed genes (DEGs) in different wheat tissues during development, relevant expression datasets available at expVIP platform were used (Ramírez-González et al. 2018; Pfeifer et al. 2014; Gillies et al. 2012; Li et al. 2013; Leach et al. 2014). Heatmaps were then generated using Morpheus (https://software.broadinstitute.org/morpheus/) to show the expression levels of genes in different wheat tissues. Among the DEGs detected, those with functions previously reported to be associated with disease resistance were also selected for the different MQTLs.

Results

Salient features of the QTLs collected for meta-analysis

A total of 493 QTLs were available from 58 studies, including 21 studies for STB, 17 for SNB, 12 for FHB, 6 for KB, and only 2 for LS published from 1998 to April 2021 (Online Resource 1, 2), which involved 62 different mapping populations including 20 DH, 39 RIL populations and 3 F2/BC populations (some

studies involved more than one populations) ranging in size from 70 to 316 lines that were evaluated each for more than one year.

The total number of QTLs was 493 (184 were associated with FHB, 126 with STB, 103 with SNB, 66 with KB, and only 14 QTLs with LS) (Fig. 1a). These QTLs were unevenly distributed on the 21 wheat chromosomes ranging from 9 QTLs on 5D to 54 on 5B (Fig. 1b) and on three sub-genomes, with 151 on sub-genome A, 232 on sub-genome B, and 110 on sub-genome D (Fig. 1b). The PVE for a single QTL ranged from 0.13 to 94.1 (average of 13.47%), with most of the QTLs showing PVE < 20% (Fig. 1c); the confidence intervals (CIs) ranged from zero to 197.6 cM, with an average of 13.57 cM (Fig. 1d). The QTL data collected in this study has been included in the recently developed WheatQTL database (http://wheatqtldb.net/) (Singh et al. 2021).

Characteristics Of The Consensus Map

The consensus map had 50,355 markers spread over a distance of 9229.87 cM (ranging from 144.41 cM for 3D to 746.98 cM for 5B with an average of 439.52 cM) (Online Resource 3). The overall marker density was 5.45 markers/cM, ranging from 1.79 markers/cM on chromosome 4D to 12.95 markers/cM on chromosome 2A (Online Resource 4). Sub-genome A contained 2,691 markers over a distance of 437.32 cM, sub-genome B carried 3287 markers over a distance of 544.39 cM and had the highest marker density (6.04 markers/cM), and sub-genome D contained 1214 markers over a distance of 336.84 cM and presented the lowest marker density (3.60 markers/cM). Overall, the marker density at the fore-end of chromosomes was considerably higher than that at the end (Fig. 2).

Qtl Projection And Meta-qtl Analysis

Only 291 QTLs of the available 493 QTLs could be projected onto the consensus map; 208 QTLs were grouped into 63 MQTLs (Table 2, S5), leaving 38 singletons (single QTLs), and 45 unassigned to any MQTL (predicted QTL peaks were outside the MQTL CI). The 63 MQTLs were distributed on the different wheat chromosomes (Fig. 3); with a maximum of 7 MQTLs on 5B and a minimum of only one MQTL each on 1D, 2A, 4A, 6D, and 7D. As many as 22 MQTLs (34.92%) were based on 4 or more initial QTLs. The CI of MQTLs ranged from 0.04 to 15.31 cM with an average of 3.09 cM (4.35-fold less than that of initial QTLs) (Fig. 4); 33 out of 63 MQTLs had CI < 2 cM. Moreover, there were substantial differences in average CIs of MQTLs among different chromosomes (Fig. 4). The PVE ranged from 2.24 to 51.23% with a mean of 15.24%; LOD score ranged from 2.93 to 48.44 with an average of 7.42. Only a solitary MQTL (MQTL2B.2) provided resistance to all the 5 diseases; each of ten MQTLs (1A.1, 1B.4, 2A.1, 2B.2, 2D.3, 3B.1, 3B.2, 3B.3, 4A.1, 4B.3, 5B.3) provided resistance to 3–4 diseases; and the remaining provided resistance each for only one disease, although there could be more than one MQTLs for the same disease (for instance, MQTL6A.2 accommodated 4 QTLs for FHB, 4B.4 carried 3 QTLs for LS, and 3A.1 carried 3 QTLs for SNB). The remaining details about MQTLs are available in Table 2.

Table 2
MQTLs associated with multiple disease resistance identified in this study

MQTL (Physical interval, in Mb)	Flanking markers (CI, in cM)	N QTLs (avg. LOD)	Trait (avg. PVE)
MQTL1A.1 (27.26–27.76)	RAC875_c16820_419/wsnp_Ra_c26191_35761997 (32.98–37.6)	4 (4.25)	STB, SNB, FHB (5.78)
MQTL1A.2 (344.69-571.29)	wsnp_Ku_c816_1684354/CAP7_c490_123 (153.25-156.23)	3 (4.17)	FHB, SNB (10.37)
MQTL1B.1 (7.83–58.06)	wsnp_RFL_Contig2449_2013497/wsnp_CAP8_c2023_1110474 (2.105–2.915)	3 (3)	SNB, STB (8.4)
MQTL1B.2 (58.06–74.29)	wsnp_Ra_c12151_19543036/wsnp_JD_rep_c63201_40318622 (5.665–7.115)	5 (6.62)	SNB, STB (18.8)
MQTL1B.3 (646.16-646.18)	CAP7_c199_62/Xabg373 (57.21–57.45)	2 (5.5)	FHB, SNB (8.65)
MQTL1B.4 (432.37-563.07)	Kukri_c147_1620/cfa2129b (66.86–68.86)	4 (8.7)	STB, LS, FHB (12.42)
MQTL1D.1 (10.26–12.31)	AX-94817725/Excalibur_c55959_710 (48.91–59.28)	2 (4.08)	STB (17.4)
MQTL2A.1 (8.35–24.29)	wPt-9793/AX-94570860 (5.67–13.19)	5 (3.96)	FHB, SNB, STB (7.86)
MQTL2B.1 (3.78–9.11)	wPt-1634/Xcfd276 (8.12–11.16)	3 (4.9)	SNB, FHB (4.8)
MQTL2B.2 (387.83-536.75)	RAC875_rep_c109471_154/Xwmc25 (57.59–58.48)	6 (6.98)	STB, FHB, STB, LS, SNB (20.8)

[#] Physical intervals of these MQTLs could not be worked out.

MQTL (Physical interval, in Mb)	Flanking markers (CI, in cM)	N QTLs (avg. LOD)	Trait (avg. PVE)
MQTL2B.3 (613.1-788.54)	BS00070900_51/Lr50 (100.3-100.48)	5 (4.05)	SNB, STB (14.64)
MQTL2B.4 (698.3-773.15)	wsnp_Ra_c14267_22357509/D_GDS7LZN01D8KK0_75 (124.98-126.72)	3 (2.93)	FHB, STB (4.8)
MQTL2D.1 (14.25–14.78)	wsnp_Ex_c7669_13090850/Xbarc90 (16.33–16.59)	2 (16.25)	SNB (23.5)
MQTL2D.2 (19.63–24.97)	wsnp_RFL_Contig1945_1118187/1091926 (22.77–24.89)	2 (5.35)	STB, SNB (7.4)
MQTL2D.3 (15.58–19.62)	Xfba88/Xfba4 (39.55–39.85)	3 (5.12)	STB, FHB, SNB (10.43)
MQTL2D.4 (561.15-574.39)	Xcfd43/wPt-0619 (52.11–52.25)	6 (10.3)	FHB, SNB (16.16)
MQTL2D.5 (642.27-648.55)	wsnp_Ra_c4712_8489753/Xfbb72a (123.17-130.83)	3 (7.8)	FHB (20.63)
MQTL3A.1 (25.36–60.2)	D_GDEEGVY02FU4W8_119/gwm369 (1.83–2.82)	3 (3.17)	SNB (7.77)
MQTL3A.2 (1.38–12.25)	Kukri_c41361_186/BS00048491_51 (44.24–45.8)	2 (5.65)	FHB (5.02)
MQTL3B.1 (18.85–29.46)	3955846/M21/P76.3 (2.22-3)	5 (8.47)	SNB, FHB, KB, STB (15.57)
MQTL3B.2 (0.21–7.61)	XksuG53/4989073 (14.79–15.07)	6 (6.99)	SNB, STB, FHB, KB (17.19)
MQTL3B.3 (77.72-201.35)	Xgwm566/Xwmc762 (61.18–76.49)	3 (5.17)	FHB, SNB, STB (9.1)

[#] Physical intervals of these MQTLs could not be worked out.

MQTL (Physical interval, in Mb)	Flanking markers (CI, in cM)	N QTLs (avg. LOD)	Trait (avg. PVE)
MQTL3B.4 (753.69-789.33)	BobWhite_c22016_155/BS00087534_51 (191.66-193.78)	2 (3.5)	FHB (7.4)
MQTL3D.1 (448.27-613.12)	IAAV5582/wsnp_Ex_rep_c101732_87042471 (9.94–10.23)	2 (3)	STB, SNB (8.9)
MQTL3D.2 (601.92–604.3)	Xgwm183a/CAP12_rep_c3953_177 (14.7-15.47)	2 (8.85)	STB (26.8)
MQTL3D.3 (587.21-611.67)	Xwmc418/Xcnl5b (44.64–45.33)	2 (3.85)	STB, KB (36.5)
MQTL4A.1 (11.36-737.38)	Excalibur_c56041_728/wsnp_BE403710B_Ta_2_1 (1.08–3.33)	5 (12.36)	FHB, STB, KB (33.14)
MQTL4B.1 (24.34–37.55)	AX-95174194/AX-94943082 (34.55–38.36)	5 (17.57)	FHB, KB (12.93)
MQTL4B.2 (14.12–16.05)	Xwmc310/GENE-4933_1176 (97.73-100.62)	2 (7.75)	SNB, STB (10.35)
MQTL4B.3 (24.55–26.49)	BS00081631_51/Tdurum_contig64772_417 (111.89-115.45)	4 (14.15)	STB, FHB, SNB (19.15)
MQTL4B.4 (618.59-621.33)	RAC875_c104178_425/Xbcd402c (141.19-141.35)	3 (3.19)	LS (2.24)
MQTL4D.1 (36.45-324.47)	Xcfd71/Xbarc0105 (3.32–7.89)	2 (6.6)	FHB, STB (11.25)
MQTL4D.2 (121.19-439.67)	Xbarc288/Kukri_rep_c68594_530 (21.39–27.61)	3 (24.17)	FHB (37.63)
MQTL4D.3 (25.99-481.55)	AX-94773648/Xcfd39b (29.55–39.97)	2 (11.5)	FHB, SNB (12.35)

[#] Physical intervals of these MQTLs could not be worked out.

MQTL (Physical interval, in Mb)	Flanking markers (CI, in cM)	N QTLs (avg. LOD)	Trait (avg. PVE)
MQTL5A.1 (5.99–19.98)	Kukri_c14683_65/RAC875_c53808_1027 (11.48–12.34)	2 (10.77)	SNB, STB (14.59)
MQTL5A.2 (132.19-165.68)	wsnp_Ex_c62351_62025537/BF202040-164 (49.1–50.6)	3 (6.57)	SNB, FHB (8.81)
MQTL5A.3 (556.68–558.9)	Xwmc150/wPt-3620 (98.10-99.29)	2 (3.72)	FHB, STB (31.46)
#MQTL5A.4	Xmwg522/Xcfa2121 (127.62-127.77)	4 (4.46)	STB, FHB (9.815)
MQTL5A.5 (623.48-630.93)	Xbarc232/Xcfa2185 (188.45-189.46)	3 (3)	FHB, KB (11.67)
MQTL5B.1 (294.08-402.79)	Xbarc74/IWB73666 (17.23–21.66)	6 (6.5)	STB, SNB (12.02)
MQTL5B.2 (436.58-481.54)	BS00023064_51/JG_c2778_160 (45.38–47.71)	5 (3.6)	KB, STB (12.92)
MQTL5B.3 (672.95–684)	XP7152-196/AX-110438459 (54.06–55.86)	3 (4.9)	KB, FHB, STB (12.33)
MQTL5B.4 (571.2-600.13)	RAC875_c52086_72/Xcfd156 (77.8-81.16)	2 (4.55)	FHB (15.1)
MQTL5B.5 (660.76-712.85)	Xgwm272/Xwmc443 (136.29-136.35)	2 (18.37)	SNB, FHB (21.12)
#MQTL5B.6	wPt-3049/TC86533 (166.29–172.70)	3 (7.42)	SNB, FHB (17.1)
MQTL5B.7 (480.48–587.6)	Excalibur_c76347_77/BobWhite_c1238_1826 (238.74-238.83)	4 (5.2)	SNB, FHB (6.16)

Physical intervals of these MQTLs could not be worked out.

MQTL (Physical interval, in Mb)	Flanking markers (CI, in cM)	N QTLs (avg. LOD)	Trait (avg. PVE)
MQTL5D.1 (61.86–75.92)	BobWhite_c1372_133/Ra_c6082_737 (33.5-33.84)	2 (3.6)	STB, SNB (21.2)
MQTL5D.2 (123.5-331.4)	Kukri_c444_833/Xcfd78 (40.35–55.66)	2 (3.7)	FHB, SNB (20)
MQTL6A.1 (11.25–11.55)	wsnp_Ku_c7471_12865509/wPt-1742 (39.84–40.19)	3 (4.35)	SNB, STB (42)
MQTL6A.2 (16.57–25.63)	Ku_c10377_335/Excalibur_c14693_724 (68.12–78.76)	4 (4.9)	FHB (9.27)
MQTL6B.1 (18.34–22.12)	RFL_Contig3110_2172/Xgwm1051 (26.06–30.25)	3 (8.13)	STB, FHB (9.17)
MQTL6B.2 (36.18–88.71)	wPt-0470/RAC875_rep_c111705_629 (85.34–91.79)	2 (3.55)	SNB, KB (3.62)
MQTL6B.3 (227.28-436.46)	wPt-9784/wPt-3060 (121.85-123.71)	3 (20)	LS, FHB (51.23)
#MQTL6D.1	P32/M52-290/XMXE3M8o (90.73-100.63)	2 (4.8)	STB (7.2)
MQTL7A.1 (9.19–21.66)	X304060/Xfba17 (0.53–3.43)	5 (3.2)	STB, FHB (9.12)
MQTL7A.2 (21.8-33.65)	AX-94785770/Ku_c416_1522 (52.97–53.57)	7 (7.47)	SNB, FHB (15.51)
MQTL7A.3 (424.65-596.71)	Xwmc179/Xgbx3480a (77.81–80.80)	3 (4.8)	FHB, KB (9.03)
MQTL7A.4 (115.2-311.91)	Lr47/BobWhite_c8796_599 (90.97–91.35)	4 (3.68)	FHB, SNB (5.38)
MQTL7B.1 (708.47-744.25)	BG262689-071/4207627|F|0–30:C > G-30:C > G (19.7-19.74)	2 (48.44)	LS, STB (47.99)

Physical intervals of these MQTLs could not be worked out.

MQTL (Physical interval, in Mb)	Flanking markers (CI, in cM)	N QTLs (avg. LOD)	Trait (avg. PVE)
MQTL7B.2 (232.75-394.11)	wsnp_CAP11_c203_195421/wsnp_RFL_Contig2148_1449634 (28.3-33.16)	5 (4.34)	FHB, SNB (10.28)
MQTL7B.3 (613.25-621.92)	Excalibur_c29455_476/wsnp_BF292987B_Td_2_1 (49.36–49.86)	2 (3)	SNB, STB (11.55)
MQTL7B.4 (719.08-744.09)	Excalibur_c1070_1978/wPt-0786 (123.03-124.85)	3 (3.37)	STB, FHB (4.03)
MQTL7D.1 (532.95-570.65)	Jagger_c1294_346/Xgwm44 (77.42–82.86)	3 (3.69)	STB, FHB (24.33)

[#] Physical intervals of these MQTLs could not be worked out.

As many as 60 MQTLs (except MQTL5A.4, 5B.6, and 6D.1) were anchored to the physical map of the wheat reference genome (Online Resource 5). The mean physical interval of MQTLs ranged from 0.30 Mb (MQTL6A.1) to 726.01 Mb (MQTL4A.1), with a mean of 74.09 Mb (31 MQTLs had < 20 Mb). The physical intervals of several MQTLs were shown to overlap, for instance, 2B.3 (613.09-788.53 Mb) and 2B.4 (698.3-773.15 Mb); 4B.1 (24.33–37.55 Mb) and 4B.3 (24.55–26.49 Mb).

Validation of MQTLs with GWAS and co-localization with different resistance genes

The physical coordinates of the above 60 MQTLs were compared with MTAs for disease resistance reported in 16 GWAS, earlier conducted in wheat (6 studies for STB, 2 studies for SNB, 3 studies for KB, and 5 studies for FHB; no GWAS for LS). Of the 60 MQTLs, 38 could be validated, each in at least one GWAS, (involving a total of 111 MTAs) (Fig. 3, Online Resource 6), among them, 22, 20, 13, and 5 MQTLs were verified using MTAs associated with FHB, STB, KB, and SNB resistance, respectively (Fig. 5). The number of MTAs for each MQTL also varied, so that as many as 15 MQTLs each matched with at least 3 MTAs identified in 16 GWA studies; of these MQTL4A.1 matched with 23 MTAs, followed by MQTL1B.1 and 1B.7 with 9 and 8 MTAs, respectively. Some of the MQTLs (e.g., MQTL2B.3, 3B.2, and 4A.1) each involving 5 or more initial QTLs matched with more than 4 MTAs (Fig. 5).

Positions of MQTLs were also compared with those of the 50 available known resistance genes (Online Resource 7). MQTLs identified in the present study overlapped 12 resistance genes [including 6 genes for STB (*Stb1*, *TaSSP6*, *Stb8*, *Stb11*, *Stb12*, and *TaSRTRG6*), 5 for FHB (*Fhb2*, *WFhb1-1*, *Tapgip3*, *TaNACL-D1*, *Ta-UGT3*), and 1 for KB (*Chs-1B*)] (Online Resource 7). For instance, MQTL1B.1 overlapped *Chs-1B* and *Stb11*, MQTL3B.3 overlapped *Tapgip3* and *Ta-UGT3* genes and MQTL2B.4 and 1B.4 overlapped two most recently cloned STB resistance genes, *TaSSP6* and *TaSRTRG6*, respectively.

Candidate Genes And Their Gene Ontology (Go) Terms

As many as 874 CGs were available in the genomic regions of 39 selected MQTLs, each based on at least three QTLs and with an average genetic and physical CIs of 2.94 cM and 81.55 Mb, respectively (Online Resource 8). These CGs included 149 genes with unknown functions. On the two extremes, MQTL2A.1 gave a maximum of 81 CGs and MQTL6B.3 gave a solitary CG. Many CGs were detected repeatedly in different MQTL regions, the frequency distributions of these CGs are presented in Fig. 6. The number of genes encoding for nucleotide-binding site leucine-rich repeat (NBS-LRR) domains or *R* genes per MQTL ranged from zero in several MQTLs to 13 in MQTL6B.1 (Online Resource 8). GO analysis suggested a variety of functions for the CGs including those involved in a variety of biological processes and molecular functions, at least some of them are associated with disease resistance (Online Resource 8).

Differentially Expressed Genes (Degs) In Mqtl Regions

In silico expression analysis was performed for a total of 453 genes detected in 20 most robust and stable MQTLs (those involving at least 4 initial QTLs) (Online Resource 8). The first transcriptomic data-set revealed 82 DEGs with 23 up-regulated genes, 50 down-regulated genes, and 9 genes that were up-regulated under some conditions and down-regulated under others (Tables S8, S9). The number of DEGs ranged from one in MQTL2B.3 to 12 in MQTL2A.1. The second dataset revealed 36 DEGs with 15 genes up-regulated, 12 genes down-regulated, and 9 genes up-regulated under some conditions and down-regulated under others. From this data-set, MQTL2A.1 had the maximum DEGs (9), while no DEG was detected for the following five MQTLs: 1A.1, 2B.3, 4B.1, 7A.4, and 7B.2 (Online Resource 9).

The third data set uncovered 32 DEGs with 10 up-regulated genes, 14 down-regulated genes, and 8 genes that were up-regulated at one time-point and down-regulated in others. Same to the first and second datasets, MQTL2A.1 had the highest number of DEGs (7), while several MQTLs including 2B.3, 4B.1, 5B.7, 7A.2, 7A.4, and 7B.2 had no DEG. The fourth data-set did not provide expression values of the CGs under control conditions, therefore, comparative evaluation (stress versus control) of the expression of the CGs could not be performed. In this case, we considered those CGs as important for the concerned disease that showed at least 2 transcripts per million (TPM) expression. As many as 108 such CGs were discovered. The fifth data-set, revealed a total of 50 DEGs, with 19 up-regulated genes and 31 down-regulated genes. From this data-set also, MQTL2A.1 had the maximum DEGs (11), while no DEG was identified for 1B.4, 2B.3, and 5B.7. A total of 25 genes were observed to be differentially expressed across three or more expression databases used (Online Resource 9).

Overall, 194 DEGs were identified for all the studied MQTLs (except MQTL4A.1) (Online Resource 9); the number of DEGs per MQTL ranged from 1 (MQTL2B.3) to 36 (MQTL2A.1). Further, these DEGs encoded different proteins belonging to the following categories: (i) R-domain containing proteins, (ii) transcription factors like NAC domain, AP2/ERF, SANT/Myb domain, Zinc finger binding domain-containing proteins, etc (iii) different protein kinases, (iv) transporters like SWEET sugar transporter, sugar/inositol transporter,

etc., (v) genes involved in oxidation-reduction reactions like cytochrome P450, (vi) genes involved in antioxidative defense, for instance, glutathione S-transferase, (vii) cupin superfamily proteins, for instance, germin like protein, (viii) invertase inhibitors like pectinesterase inhibitor, etc., (ix) glycosyltransferase enzymes, for instance, UDP-glucuronosyl/UDP-glucosyltransferase, and (x) WD40 repeat proteins. Among the DEGs detected, those with functions earlier reported as important for disease resistance were considered the most promising CGs for individual MQTLs. As many as 85 such CGs were available from 18 MQTLs (Table 3); these are listed in Table 3 along with their GO terms.

Table 3
High confidence MQTLs and their CGs that exhibited differential gene expression during the *in silico* expression analysis

MQTL (Total CGs identified; DEGs)	Important CGs	Functional annotation	Gene ontology term
MQTL1A.1 (13; 7)	TraesCS1A02G045700	Glutathione S-transferase	glutathione dehydrogenase activity
MQTL1A.1	TraesCS1A02G046300	NUDIX hydrolase domain	hydrolase activity
MQTL1A.1	TraesCS1A02G046400	PMR5 N-terminal domain	-
MQTL1A.1	TraesCS1A02G047000	P-type ATPase	integral component of membrane
MQTL1B.2 (13; 4)	TraesCS1B02G081900	Glycosyl transferase	integral component of membrane
MQTL1B.2	TraesCS1B02G082900	Ankyrin repeat-containing domain	-
MQTL1B.4 (8; 4)	TraesCS1B02G286300	Cytochrome P450	heme binding
MQTL1B.4	TraesCS1B02G286600	G10 protein	nucleus
MQTL1B.4	TraesCS1B02G285900	Zinc finger C2H2-type	nucleic acid binding
MQTL1B.4	TraesCS1B02G286500	Ribosomal protein L12 family	structural constituent of ribosome
MQTL2A.1 (80; 36)	TraesCS2A02G036100	Pectinesterase inhibitor domain	enzyme inhibitor activity
MQTL2A.1	TraesCS2A02G036300	Thiolase	transferase activity
MQTL2A.1	TraesCS2A02G036500	Adenylate kinase/UMP-CMP kinase	ATP binding
MQTL2A.1	TraesCS2A02G037600	Serpin family	extracellular space
MQTL2A.1	TraesCS2A02G038300-38400	Glycoside hydrolase	hydrolase activity
MQTL2A.1	TraesCS2A02G039300	Zinc finger, RING-CH-type	integral component of membrane
MQTL2A.1	TraesCS2A02G039400	Glycoside hydrolase	hydrolase activity
MQTL2A.1	TraesCS2A02G040000	NB-ARC	ADP binding
MQTL2A.1	TraesCS2A02G040200	Proteasome component (PCI) domain	cytoplasm
MQTL2A.1	TraesCS2A02G040900-41000	Protein kinase domain	ATP binding

MQTL (Total CGs identified; DEGs)	Important CGs	Functional annotation	Gene ontology term
MQTL2A.1	TraesCS2A02G041300-41400	Amidase	amidase activity
MQTL2A.1	TraesCS2A02G042400-42500	NB-ARC	ADP binding
MQTL2A.1	TraesCS2A02G043200	SWEET sugar transporter	integral component of membrane
MQTL2B.2 (16; 9)	TraesCS2B02G322800	Glutathione S-transferase	protein binding
MQTL2B.2	TraesCS2B02G323500	NAC domain	nucleus
MQTL2B.2	TraesCS2B02G323700	Protein kinase domain	ATP binding
MQTL2B.2	TraesCS2B02G324200	Glycolipid transfer protein domain	cytoplasm
MQTL2B.2	TraesCS2B02G324300	Zinc finger, CCCH-type	metal ion binding
MQTL2D.4 (26; 11)	TraesCS2D02G461500	NSF attachment protein	intracellular protein transport
MQTL2D.4	TraesCS2D02G461700	Myc-type, basic helix-loop-helix (bHLH) domain	protein dimerization activity
MQTL2D.4	TraesCS2D02G461000	Pentatricopeptide repeat	zinc ion binding
MQTL2D.4	TraesCS2D02G460100	Germin	extracellular region
MQTL2D.4	TraesCS2D02G462300	Protein kinase domain	integral component of membrane
MQTL3B.1 (34; 16)	TraesCS3B02G045900	CALMODULIN-BINDING PROTEIN60	calmodulin binding
MQTL3B.1	TraesCS3B02G046100	Fatty acid hydroxylase	integral component of membrane
MQTL3B.1	TraesCS3B02G047500	AAA + ATPase domain	ATP binding
MQTL3B.1	TraesCS3B02G049100	Protein kinase domain	ATP binding
MQTL3B.2 (53; 22)	TraesCS3B02G005000-5100	Protein kinase domain	ATP binding
MQTL3B.2	TraesCS3B02G005900	Histone deacetylase interacting domain	cytoplasm
MQTL3B.2	TraesCS3B02G006600	Cytochrome P450	diacylglycerol O-acyltransferase activity
MQTL3B.2	TraesCS3B02G006700	O-acyltransferase	integral component of membrane

MQTL (Total CGs identified; DEGs)	Important CGs	Functional annotation	Gene ontology term
MQTL3B.2	TraesCS3B02G008200	Pectinesterase inhibitor domain	ATP binding
MQTL3B.2	TraesCS3B02G008600	Protein kinase domain	enzyme inhibitor activity
MQTL3B.2	TraesCS3B02G008900	Pectinesterase inhibitor domain	-
MQTL3B.2	TraesCS3B02G009600	Lysine-rich arabinogalactan protein 19	serine-type endopeptidase inhibitor activity
MQTL3B.2	TraesCS3B02G009700	Proteinase inhibitor I13	-
MQTL4B.1 (14; 9)	TraesCS4B02G042900	Zinc finger, RING-type	integral component of membrane
MQTL4B.1	TraesCS4B02G043100	GRAS TF	protein binding
MQTL4B.1	TraesCS4B02G043200	Tetratricopeptide-like helical domain superfamily	calcium ion binding
MQTL4B.1	TraesCS4B02G043300	Phospholipase A2	plasma membrane
MQTL4B.3 (40; 24)	TraesCS4B02G032800	ATP-dependent RNA helicase DEAD-box	-
MQTL4B.3	TraesCS4B02G033100-33600	Germin	extracellular region
MQTL4B.3	TraesCS4B02G033700	Ankyrin repeat	structural constituent of ribosome
MQTL4B.3	TraesCS4B02G033900	Ribosomal protein S21	structural constituent of ribosome
MQTL4B.3	TraesCS4B02G034400	Ribosomal protein L18	cytoplasm
MQTL4B.3	TraesCS4B02G035100	Leucine-rich repeat	chloroplast thylakoid membrane
MQTL4B.3	TraesCS4B02G035400	Proteasome	integral component of membrane
MQTL4B.3	TraesCS4B02G035500	CBS domain	integral component of membrane
MQTL5B.1 (11; 5)	TraesCS5B02G192700	DnaJ domain	copper ion homeostasis
MQTL5B.1	TraesCS5B02G193200	AP2/ERF domain	carbohydrate metabolic process

MQTL (Total CGs identified; DEGs)	Important CGs	Functional annotation	Gene ontology term
MQTL5B.2 (15; 5)	TraesCS5B02G272600	Glycoside hydrolase	nucleus
MQTL5B.2	TraesCS5B02G272800	WD40 repeat	-
MQTL5B.2	TraesCS5B02G274000	P-loop containing nucleoside triphosphate hydrolase	ATP binding
MQTL5B.7 (18; 2)	TraesCS5B02G355100	Protein kinase domain	nucleus
MQTL5B.7	TraesCS5B02G354800	High mobility group box domain	protein binding
MQTL6A.2 (29; 8)	TraesCS6A02G039200	WD40 repeat	nucleus
MQTL6A.2	TraesCS6A02G040200-40500	Histone H2B	DNA binding
MQTL6A.2	TraesCS6A02G040900	F-box domain	nucleic acid binding
MQTL7A.1 (24; 9)	TraesCS7A02G033500	Guanine nucleotide binding protein	catalytic activity
MQTL7A.1	TraesCS7A02G034300	Glutathione S-transferase	protein binding
MQTL7A.1	TraesCS7A02G034500	Glutathione S-transferase	protein binding
MQTL7A.1	TraesCS7A02G035400	F-box-like domain superfamily	nucleus
MQTL7A.1	TraesCS7A02G036100	SANT/Myb domain	cytoplasm
MQTL7A.2 (36; 14)	TraesCS7A02G055400	Ubiquitin-like domain	transferase activity
MQTL7A.2	TraesCS7A02G055800	UDP-glucuronosyl/UDP-glucosyltransferase	transferase activity
MQTL7A.2	TraesCS7A02G056200	UDP-glucuronosyl/UDP-glucosyltransferase	integral component of peroxisomal membrane
MQTL7A.2	TraesCS7A02G056600-56700	Glutathione S-transferase	integral component of membrane
MQTL7A.2	TraesCS7A02G056800	Protein kinase domain	transferase activity
MQTL7A.2	TraesCS7A02G057100	BTB/POZ domain	DNA-binding TF activity
MQTL7A.2	TraesCS7A02G057700-57800	AP2/ERF domain	DNA-binding TF activity

MQTL (Total CGs identified; DEGs)	Important CGs	Functional annotation	Gene ontology term
MQTL7A.4 (8; 4)	TraesCS7A02G239500	Transcription factor CBF/NF-Y/archaeal histone domain	integral component of membrane
MQTL7A.4	TraesCS7A02G239900	Nonaspanin	DNA-binding TF activity
MQTL7B.2 (5; 3)	TraesCS7B02G186900	AP2/ERF domain	nucleic acid binding
MQTL7B.2	TraesCS7B02G187000	ATP-dependent RNA helicase DEAD-box	metal ion binding
MQTL7B.2	TraesCS7B02G187100	Zinc finger, CCCH-type	

The expression patterns of all the 194 DEGs across different tissues at different wheat development stages were also analyzed. Column clustering was performed, and consequently, the 194 DEGs were grouped into two classes based on their expression patterns in different tissues. The expression patterns of some selected CGs in different wheat tissues are shown in Fig. 7. Genes in class I showed high expression in the roots and leaves/shoots at vegetative stages when compared to other stages of growth (Fig. 7). Class I included the genes (encoding mainly for protein kinases, glutathione S-transferase, ankyrin repeat-containing domain, G10 protein, Thiolase, Zinc finger, NAC domain, calmodulin-binding protein, and germin-like protein, etc.). Whereas, genes from Class II showed high expression mainly in the spike (including stamen, rachis, stigma, pistil, and ovary, etc.) and grains (including seed coat, endosperm, embryo, and aleurone layer, etc.) (Fig. 7). Following are some examples of class II genes-cytochrome P450, Pectinesterase inhibitors, and SWEET sugar transporter.

Discussion

In wheat, QTLs and *R* genes for disease resistance have been identified against almost all important pathogens, including biotrophs, necrotrophs, and hemi-biotrophs. For, necrotrophs, sensitivity genes (*S* genes) are also known so that recessive alleles of these *S* genes can also be used for providing resistance (Gupta et al. 2021b). The QTLs have already been identified using interval mapping involving different types of mapping populations (mainly DH and RILs). Most of these mapping studies have each largely focused on a single disease and there are only a few papers available where individual QTLs, each conferring resistance to more than one disease, are available (Hernandez et al. 2012; Jighly et al. 2016; Zwart et al. 2010; Mago et al. 2011). Availability of individual MQTLs each for more than one disease, as observed in the present study, is yet another evidence for the MDR hypothesis (Wiesner-Hanks and Nelson, 2016). Like the present study, meta-QTL analysis for MDR has also been conducted in several other crops including barley, maize, and rice (Wisser et al. 2005; Kumar et al. 2020; Schweizer and Stein, 2011; Ali et al. 2013).

This motivated us to perform a genome-wide meta-analysis on previously identified QTLs associated with five important diseases, including STB, SNB, FHB, KB, and LS in wheat. To our knowledge, the present study is the first report of meta-QTL analysis for MDR in wheat, although individual QTLs for MDR have been reported. A characteristic of the QTL database and consensus map used in the present study was that the B sub-genome had the highest marker density, and therefore, carried the maximum number of QTLs, with the D sub-genome contained the minimum number of QTLs. This feature of the meta-QTL analysis is in agreement with several earlier studies on meta-QTL analysis for resistance against a number of individual diseases in wheat (Goudemand et al. 2013; Soriano and Royo, 2015; Venske et al. 2019; Liu et al. 2019; Zheng et al. 2020; Jan et al. 2021; Aduragbemi and Soriano, 2021).

In the present study, more than 80 % (51/63) of MQTLs were involved in providing resistance to at least two of the five diseases studied; some of these MQTLs (e.g., 2B.2, 3B.1) were associated with resistance to diverse pathogens with a range of lifestyles (necrotrophic, hemibiotrophic and biotrophic), whereas others (e.g., 1A.2, 1B.3, 2B.1) were associated with resistance only to necrotrophs. These MQTLs for MDR can be used to provide resistance against multiple diseases. The phenomenon of co-localization of QTLs for MDR in wheat was also discovered in an earlier study, where 13 QTLs spread over on nine wheat chromosomes were significantly associated with resistance to four different diseases viz., stripe rust, leaf rust, tan spot, and karnal bunt (Hernandez et al. 2012). In another study, Zwart et al. (2010) identified a QTL representing a cluster of tightly linked loci on chromosome 3D for resistance against a number of foliar diseases (STB, tan spot, stripe rust, leaf rust, and stem rust). It is thus obvious that although individual QTLs for MDR were known, no earlier report on meta QTL analysis for MDR is available in wheat.

The MDR at the level of individual QTLs/genes or MQTLs can be explained based on pleiotropic effects or clusters of tightly linked QTLs/genes. The closely linked multiple QTLs may be available either in the coupling or in the repulsion phase resulting in positive and negative correlations between resistance against more than one disease. For instance, the wheat *Sr2* locus, which provides resistance to stem rust, leaf rust, and powdery mildew (Mago et al. 2011), was tightly linked in the repulsion phase to the *Fhb1* locus, which confers resistance to FHB (Flemmig, 2012). Similarly, resistance QTLs for STB and yellow leaf spot, inherited from one parent, were linked in repulsion to *Lr24/Sr24* locus conferring resistance to leaf rust and stem rust, which was inherited from the other parent (Zwart et al. 2010). QTLs may be introgressed easily if they are linked in the coupling phase and introgression may be comparatively difficult if they are linked in the repulsion phase. It is thus obvious that to make efficient use of a resistance source, it is necessary to have a thorough understanding of its inheritance.

The results of the present study involving the validation of only 63% MQTLs with the earlier reports of GWAS are not different from the results of an earlier report, where 61.3% MQTL were validated with the results of GWAS (Yang et al. 2021). However, the results of these two studies are in disagreement with the results of another study, where only 38.66% MQTLs were supported by the GWAS data (Aduragbemi and Soriano, 2021). These widely different results are not a surprise, because the materials used for meta-

QTL analysis and GWAS often differed significantly and might involve different levels of genetic variation.

Some of the MQTLs identified during the present study also overlap individual wheat resistance genes. Following are some examples: (i) MQTL6B.3 identified during the present study overlaps *Fhb2*, which is known to confer resistance against four different traits including disease severity, disease incidence, visual rating index, and f*usarium* damaged kernels associated with FHB resistance (Cuthbert et al. 2007). (ii) MQTL3B.2 overlaps the gene *WFhb1-1 (already cloned)*, which encodes a putative membrane protein, and its overexpression caused a significant decrease in fusarium-diseased kernel rate, fusarium-damaged rachis rate, and deoxynivalenol (DON) content in harvested wheat grains (Paudel et al. 2020). (iii) MQTL3B.3 is co-localized with two FHB resistance genes (*Ta-UGT3* and *Tapgip3*), although the association between these two genes has never been examined. The gene *Tapgip3* encodes for polygalacturonase-inhibiting protein which can detect and inhibit polygalacturonase (a hydrolase released by fungi to infect plants) hence, protects plants from fungal infection by lowering polygalacturonase hydrolytic activity (Hou et al. 2015). The MQTL3B.3 is found to be associated with resistance against *FHB, SNB, STB* diseases, which suggests that the genes, *Ta-UGT3 and Tapgip3* may also be effective against other fungal diseases, such as SNB and STB in addition to FHB disease. Transgenic lines overexpressing the gene *Ta-UGT3* also exhibited resistance against FHB in wheat; this gene is believed to regulate defense-related and DON-induced downstream genes (Xing et al. 2018). (iv) MQTL5D.2 is co-localized with gene *TaNACL-D1*, which encodes a protein which by interacting with a taxonomically restricted orphan protein confers resistance against FHB disease in wheat (Perochon et al. 2019). (v) MQTL1B.1 is co-localized with two genes viz., *Chs-1B* and *Stb11*, which provide resistance against KB and STB, respectively. In the present study, MQTL1B.1 was found to be associated with SNB and STB resistance, thus making this region a hotspot for selecting resistance against at least three diseases (viz., SNB, STB, and KB) in wheat.

It is also known that a given MDR locus can be either simple (when a single gene underlies an MDR locus) or complex (when several genes underlie an MDR locus) (Hulbert et al. 2001; Cooley et al. 2000). Fine-mapping studies have shown that clusters of homologous R genes frequently underlie resistance loci, including MDR loci (Michelmore and Meyers, 1998; Hulbert et al. 2001; Andersen et al. 2020). The results of the present study involving 874 CGs could also be examined in the context of MDR; 725 of these genes are known to encode different proteins, at least some of them are relevant for resistance. These genes also include genes encoding proteins, which suggest their resemblance with 48 *R* genes, which often occur in clusters and overlap the following genomic regions occupied by MQTL2A.1, 4B.3, 6B.1, and 7A.1.

Keeping in view the occurrence of *R* gene clusters in plant genomes and some examples of *R* gene clusters at MDR loci, we anticipate that more MDR loci will eventually be described by clusters of closely linked *R* genes. *R* genes within a cluster can confer resistance to distantly related pathogen taxa because sequence changes between closely related members (e.g., homologs or even paralogs) of multigene families can generate novel specificities (Michelmore and Meyers, 1998; Ashfield et al. 2012). For

instance, the two homologs of the *Arabidopsis* HRT/RPP8 gene family confer resistance to *Peronospora parasitica* and turnip crinkle virus, respectively (Cooley et al. 2000). Similarity, in *Arabidopsis*, different members of an extensive cluster of disease-resistance loci known as multiple resistance complex J (*MRC-J*) is known to confer resistance to several viruses, bacteria, an oomycete, and a fungus (Cooley et al. 2000; Gassmann et al. 1999; Narusaka et al. 2004; Takahashi et al. 2002), which also contains several other resistance gene homologs that are yet to be characterized.

The differential expression of CGs (DEGs) observed during the present study agrees with earlier studies (Jan et al 2021; Aduragbemi and Soriano, 2021). Further, the DEGs encoded different proteins, of which at least some are known to confer resistance to different diseases in crop plants; these proteins include the following: R-domain containing proteins (Dang et al. 2019; Kaur et al. 2021), transcription factors (Akio Amorim et al. 2017), protein kinases (Meng and Zhang, 2013), sugar transporters (Moore et al. 2015), genes involved in oxidation-reduction reactions (Gunupuru et al. 2018), and antioxidative defense (Gullner et al. 2018). This indicates that the *R* genes are not the only gene family involved in MDR and that numerous other gene families may also play a role in controlling multiple diseases.

Some of the important CGs which were detected during the present study may be validated or functionally characterized using different approaches like overexpression, gene editing, knockout strategies, or CG-based association mapping. Reports are also available where some of these approaches have been used for the validation of genes for their role in MDR. For instance, overexpression of the *Lr34res* multi-pathogen resistance gene encoding an ABC transporter protein conferred resistance against rust and anthracnose diseases in sorghum (Schnippenkoetter et al. 2017). Similarly, in another study, CRISPR/Cas9 based genome editing technique was used to target tomato gene *SlDmr6-1 encoding protein* belonging to 2-oxoglutarate Fe(II) dependent oxygenases; these oxygenases provide broad-spectrum resistance against multiple pathogens including, *Pseudomonas syringae*, *Phytophthora capsici*, and *Xanthomonas spp.* in tomato (de Toledo Thomazella et al. 2016).

In breeding programmes, two types of disease resistance are considered: race-specific or all-stage resistance (ASR) and race non-specific and durable resistance or APR. A study of the expression of CGs across different tissues and developmental stages can help us figure out whether the gene has a role in ASR or APR. Keeping this in view, the CGs identified in the present study were grouped into two classes based on their expression patterns in different tissues. Class I included the genes (encoding mainly for protein kinases, glutathione S-transferase, ankyrin repeat-containing domain, G10 protein, and thiolase, etc.) which are believed to govern the detection and activation of different physiological and developmental signals, particularly those involved in defense or plant-pathogen interactions, inferring their roles in seedling resistance or ASR (Garcia et al. 2012; AbuQamar et al. 2008; Gullner et al. 2018; Aduragbemi and Soriano, 2021; Lv et al. 2019; Manosalva et al. 2009). Class II included genes, which showed high expression mainly in the spike and grains suggesting their association with APR (Fig. 7). Following are some examples of class II genes encoding proteins involved in APR in different crops: cytochrome P450 (Gunupuru et al. 2018), Pectinesterase inhibitors (Marzin et al. 2016), and SWEET

sugar transporter (Moore et al. 2015). Further, the combination of seedling resistance and adult plant resistance has been shown to confer prolonged resistance over several years (Figlan et al. 2020).

Concluding Remarks

In the present study, we integrated the results of QTL mapping studies on STB, SNB, FHB, KB, and LS resistance leading to the identification of 63 MQTLs for MDR. More than half of these MQTLs were also validated using the results from GWAS. As many as 12 known major resistance genes were also found to be co-located with some of these MQTLs. Although there was only one MQTL (2B.2) providing resistance for all the five diseases, there were at least ten MQTLs that were involved in providing resistance against three or four diseases. This result will be useful for developing resistance to multiple diseases through the introgression of promising MQTLs into elite wheat germplasm and accelerate breeding for enhanced MDR. A fairly large number of *R* genes and defense genes were also identified within these MQTL regions; of these CGs, as many as 194 genes showed differential expressions across different transcriptomic datasets investigated; based on expression studies, 85 promising genes were selected and recommended for future basic studies. The results of the present study may support the improvement in breeding strategies for MDR.

Declarations

Acknowledgments

The Department of Science and Technology (DST), New Delhi, India, provided DKS with an INSPIRE fellowship, while the Head, Department of Plant Breeding and Genetics, Punjab Agricultural University, Ludhiana, India, provided the necessary facilities.

Authors' contributions

PKG and PS conceived and planned the study. AC and NP collected the literature and tabulated the data for meta-QTL analysis. DKS conducted the analysis. DKS and AC interpreted the results and wrote the manuscript. PKG and PS edited and finalized the manuscript with the help of DKS.

Funding

This research received no external funding.

Conflicts of interest/Competing interests

There are no competing interests declared by the authors.

Availability of data and material

Data generated or analyzed during this study is included in this published article (and its Supplementary Material).

Code availability

Not applicable

Ethics approval

Not applicable

Consent to participate

Not applicable

Consent for publication

Not applicable

Supplementary Information

Online Resource 1 Summary of the QTL studies used for meta-QTL analysis

Online Resource 2 QTLs used for the present study

Online Resource 3 Consensus map constructed for the meta-QTL analysis

Online Resource 4 Salient features of the newly constructed consensus map

Online Resource 5 MQTLs identified in the present study

Online Resource 6 Comparison of MQTLs with MTAs derived from GWAS

Online Resource 7 Comparison of known disease resistance genes with MQTLs

Online Resource 8 Candidate genes identified within the MQTL regions

Online Resource 9 Differentially expressed candidate genes identified in the present study

References

1. AbuQamar S, Chai MF, Luo H, Song F, Mengiste T (2008) Tomato protein kinase 1b mediates signaling of plant responses to necrotrophic fungi and insect herbivory. Plant Cell 20:1964-1983. https://doi.org/10.1105/tpc.108.059477
2. Aduragbemi A, Soriano JM (2021) Unravelling consensus genomic regions conferring leaf rust resistance in wheat via meta-QTL analysis. *BioRxiv* https://doi.org/10.1101/2021.05.11.443557

3. Akio Amorim LL, da Fonseca dos Santos R, Pacifico Bezerra Neto J, Guida-Santos M, Crovella S, Maria Benko-Iseppon A (2017) Transcription factors involved in plant resistance to pathogens. Curr Protein Pept Sci 18:335-351.
4. Ali F, Pan Q, Chen G, Zahid KR, Yan J, (2013) Evidence of multiple disease resistance (MDR) and implication of meta-analysis in marker assisted selection. PLoS One 8:pe68150. https://doi.org/10.1371/journal.pone.0068150
5. Andersen EJ, Nepal MP, Purintun JM, Nelson D, Mermigka G, Sarris PF (2020) Wheat disease resistance genes and their diversification through integrated domain fusions. Front Genet 11:p898. https://doi.org/10.3389/fgene.2020.00898
6. Arcade A, Labourdette A, Falque M, Mangin B, Chardon F, Charcosset A, Joets J (2004) BioMercator: integrating genetic maps and QTL towards discovery of candidate genes. Bioinformatics 20:2324-2326. https://doi.org/10.1093/bioinformatics/bth230
7. Ashfield T, Egan AN, Pfeil BE et al (2012) Evolution of a complex disease resistance gene cluster in diploid Phaseolus and tetraploid Glycine. Plant Physiol159:336-354. https://doi.org/10.1104/pp.112.195040
8. Buhrow LM, Cram D, Tulpan D, Foroud NA, Loewen MC (2016) Exogenous abscisic acid and gibberellic acid elicit opposing effects on *Fusarium graminearum* infection in wheat. Phytopathology 106:986-996. https://doi.org/10.1094/PHYTO-01-16-0033-R
9. Cai J, Wang S, Su Z, Li T, Zhang X, Bai G (2019) Meta-analysis of QTL for Fusarium head blight resistance in Chinese wheat landraces. Crop J 7:784-798. https://doi.org/10.1016/j.cj.2019.05.003
10. Cavanagh CR, Chao S, Wang S et al (2013) Genome-wide comparative diversity uncovers multiple targets of selection for improvement in hexaploid wheat landraces and cultivars. Proc Natl Acad Sci 110:8057-8062. https://doi.org/10.1073/pnas.1217133110
11. Chardon F, Virlon B, Moreau L et al (2004) Genetic architecture of flowering time in maize as inferred from quantitative trait loci meta-analysis and synteny conservation with the rice genome. Genetics 168:2169-2185.https://doi.org/10.1534/genetics.104.032375
12. Cooley MB, Pathirana S, Wu HJ, Kachroo P, Klessig DF (2000) Members of the Arabidopsis HRT/RPP8 family of resistance genes confer resistance to both viral and oomycete pathogens. Plant Cell 12:663-676. https://doi.org/10.1105/tpc.12.5.663
13. Cuthbert PA, Somers DJ, Brulé-Babel A (2007) Mapping of *Fhb2* on chromosome 6BS: a gene controlling Fusarium head blight field resistance in bread wheat (*Triticum aestivum* L). Theor Appl Genet 114:429-437. 10.1007/s00122-006-0439-3
14. Dang PM, Lamb MC, Bowen KL, Chen CY (2019) Identification of expressed *R*-genes associated with leaf spot diseases in cultivated peanut. Mol Biol Rep 46:225-239. https://doi.org/10.1007/s11033-018-4464-5
15. Darvasi A, Soller M (1997) A simple method to calculate resolving power and confidence interval of QTL map location. Behav Genet 27:125-132. https://doi.org/10.1023/A:1025685324830

16. de Toledo Thomazella DP, Brail Q, Dahlbeck D, Staskawicz B (2016) CRISPR-Cas9 mediated mutagenesis of a DMR6 ortholog in tomato confers broad-spectrum disease resistance. BioRxiv p064824 https://doi.org/10.1101/064824
17. Duveiller E, Singh RP, Nicol JM (2007) The challenges of maintaining wheat productivity: pests diseases and potential epidemics. Euphytica 157:417-430. https://doi.org/10.1007/s10681-007-9380-z
18. Endelman JB, Plomion C (2014) LPmerge: an R package for merging genetic maps by linear programming. Bioinformatics 30:1623-1624. https://doi.org/10.1093/bioinformatics/btu091
19. Figlan S, Ntushelo K, Mwadzingeni L, Terefe T, Tsilo TJ, Shimelis H (2020) Breeding wheat for durable leaf rust resistance in Southern Africa: variability distribution current control strategies challenges and future prospects. Front Plant Sci 11:549. https://doi.org/10.3389/fpls.2020.00549
20. Flemmig EL (2012) Molecular markers to deploy and characterize stem rust resistance in wheat MS Thesis N C State Univ Raleigh
21. Garcia AV, Al-Yousif M, Hirt H (2012) Role of AGC kinases in plant growth and stress responses. Cell Mol Life Sci 69:3259-3267. https://doi.org/10.1007/s00018-012-1093-3
22. Gassmann W, Hinsch ME, Staskawicz BJ (1999) The Arabidopsis RPS4 bacterial-resistance gene is a member of the TIR-NBS-LRR family of disease-resistance genes. Plant J 20:265-277. https://doi.org/10.1046/j.1365-313X.1999.00600.x
23. Gillies SA, Futardo A, Henry RJ (2012) Gene expression in the developing aleurone and starchy endosperm of wheat. Plant Biotechnol J10:668-679. https://doi.org/10.1111/j.1467-7652.2012.00705.x
24. Goffinet B, Gerber S (2000) Quantitative trait loci: a meta-analysis. Genetics 155:463-473. https://doi.org/10.1093/genetics/155.1.463
25. Gou L, Hattori J, Fedak G, Balcerzak M, Sharpe A, Visendi P, Edwards D, Tinker N, Wei YM, Chen GY, Ouellet T (2016) Development and validation of *Thinopyrum elongatum*–expressed molecular markers specific for the long arm of chromosome 7E. Crop Sci 56:354-364. https://doi.org/10.2135/cropsci2015.03.0184
26. Goudemand E, Laurent V, Duchalais L, Ghaffary SMT, Kema GH, Lonnet P, Margalé E, Robert O (2013) Association mapping and meta-analysis: two complementary approaches for the detection of reliable Septoria tritici blotch quantitative resistance in bread wheat (*Triticum aestivum* L). Mol Breed 32:563-584. https://doi.org/10.1007/s11032-013-9890-4
27. Gullner G, Komives T, Király L, Schröder P (2018) Glutathione S-transferase enzymes in plant-pathogen interactions. Front Plant Sci 9:1836. https://doi.org/10.3389/fpls.2018.01836
28. Gunupuru LR, Arunachalam C, Malla KB, Kahla A, Perochon A, Jia J, Thapa G, Doohan FM (2018) A wheat cytochrome P450 enhances both resistance to deoxynivalenol and grain yield. PloS one 13:0204992 https://doi.org/10.1371/journal.pone.0204992
29. Guo B, Sleper DA, Lu P, Shannon JG, Nguyen HT, Arelli PR (2006) QTLs associated with resistance to soybean cyst nematode in soybean: meta-analysis of QTL locations. Crop Sci 46:595.

10.2135/cropsci2005.04-0036-2

30. Gupta PK, Balyan HS, Chhuneja P et al (2021) Pyramiding of Genes for Grain Protein Content, Grain Quality and Rust Resistance in Eleven Indian Bread Wheat Cultivars: A Multi-Institutional Effort. 10.21203/rs.3.rs-637558/v1
31. Gupta PK, Vasistha NK, Singh PK (2021b) Sensitivity genes in wheat and corresponding effector genes in necrotrophs exhibiting inverse gene-for-gene relationship. https://doi.org/10.21203/rs.3.rs-223024/v1
32. Hernandez MV, Crossa J, Singh PK, Bains NS, Singh K, Sharma I (2012) Multi-trait and multi-environment QTL analyses for resistance to wheat diseases. PLoS One 7:pe38008. https://doi.org/10.1371/journal.pone.0038008
33. Hou W, Mu J, Li A, Wang H, Kong L (2015) Identification of a wheat polygalacturonase-inhibiting protein involved in Fusarium head blight resistance. Eur J Plant Pathol 141:731-745. https://doi.org/10.1007/s10658-014-0574-7
34. Hulbert SH, Webb CA, Smith SM, Sun Q (2001) Resistance gene complexes: evolution and utilization. Annu Rev Phytopathol 39:285-312. https://doi.org/10.1146/annurev.phyto.39.1.285
35. Jan I, Saripalli G, Kumar K et al (2021) Meta-QTL Analysis for Stripe Rust Resistance in Wheat. https://doi.org/10.21203/rs.3.rs-380807/v1
36. Jighly A, Alagu M, Makdis F, Singh M, Singh S, Emebiri LC, Ogbonnaya FC (2016) Genomic regions conferring resistance to multiple fungal pathogens in synthetic hexaploid wheat. Mol Breed 36:1-19. https://doi.org/10.1007/s11032-016-0541-4
37. Kaur B, Bhatia D, Mavi GS (2021) Eighty years of gene-for-gene relationship and its applications in identification and utilization of R genes. J Genet 100:1-17. https://doi.org/10.1007/s12041-021-01300-7
38. Knox RE, Campbell HL, Clarke FR et al (2014) Quantitative trait loci for resistance in wheat (*Triticum aestivum*) to Ustilago tritici. Can J Plant Pathol 36:187-201. https://doi.org/10.1080/07060661.2014.905497
39. Kou Y, Wang S (2010) Broad-spectrum and durability: understanding of quantitative disease resistance. Curr Opin Plant Biol 13:181-185. https://doi.org/10.1016/j.pbi.2009.12.010
40. Kugler KG, Siegwart G, Nussbaumer T et al (2013) Quantitative trait loci-dependent analysis of a gene co-expression network associated with Fusarium head blight resistance in bread wheat (*Triticum aestivum* L). BMC genomics 14:1-15. https://doi.org/10.1186/1471-2164-14-728
41. Kumar IS, Nadarajah K (2020) A meta-analysis of quantitative trait loci associated with multiple disease resistance in rice (*Oryza sativa* L). Plants 9:1491. https://doi.org/10.3390/plants9111491
42. Leach LJ, Belfield EJ, Jiang C, Brown C, Mithani A, Harberd NP (2014) Patterns of homoeologous gene expression shown by RNA sequencing in hexaploid bread wheat. BMC genomics 15:1-19. https://doi.org/10.1186/1471-2164-15-276
43. Li HZ, Gao X, Li XY, Chen QJ, Dong J, Zhao WC (2013) Evaluation of assembly strategies using RNA-seq data associated with grain development of wheat (*Triticum aestivum* L). PlOS one 8:pe83530.

https://doi.org/10.1371/journal.pone.0083530

44. Liu S, Hall MD, Griffey CA, McKendry AL (2009) Meta-analysis of QTL associated with Fusarium head blight resistance in wheat. Crop Sci 49:1955-1968. https://doi.org/10.2135/cropsci2009.03.0115
45. Löffler M, Schön CC, Miedaner T (2009) Revealing the genetic architecture of FHB resistance in hexaploid wheat (*Triticum aestivum* L) by QTL meta-analysis. Mol Breed 23:473-488. https://doi.org/10.1007/s11032-008-9250-y
46. Lv T, Li X, Fan T, Luo H, Xie C, Zhou Y, Tian CE (2019) The calmodulin-binding protein IQM1 interacts with CATALASE2 to affect pathogen defense. Plant Physiol 181:1314-1327. https://doi.org/10.1104/pp.19.01060
47. Mago R, Tabe L, McIntosh RA, Pretorius Z et al (2011) A multiple resistance locus on chromosome arm 3BS in wheat confers resistance to stem rust (Sr2) leaf rust (Lr27) and powdery mildew. Theor Appl Genet 123:615-623. https://doi.org/10.1007/s00122-011-1611-y
48. Manosalva PM, Davidson RM, Liu B, Zhu X, Hulbert SH, Leung H, Leach JE (2009) A germin-like protein gene family functions as a complex quantitative trait locus conferring broad-spectrum disease resistance in rice. Plant Physiol 149:286-296. https://doi.org/10.1104/pp.108.128348
49. Marone D, Russo MA, Laidò G, De Vita P, Papa R, Blanco A, Gadaleta A, Rubiales D, Mastrangelo AM (2013) Genetic basis of qualitative and quantitative resistance to powdery mildew in wheat: from consensus regions to candidate genes. BMC genomics 14:1-17. https://doi.org/10.1186/1471-2164-14-562
50. Marzin S, Hanemann A, Sharma S, Hensel G, Kumlehn J, Schweizer G, Röder MS (2016) Are PECTIN ESTERASE INHIBITOR genes involved in mediating resistance to Rhynchosporium commune in barley? PloS one 11:pe0150485. https://doi.org/10.1371/journal.pone.0150485
51. Meng X, Zhang S (2013) MAPK cascades in plant disease resistance signalling. Annu Rev Phytopathol 51:245-266. https://doi.org/10.1146/annurev-phyto-082712-102314
52. Michelmore RW, Meyers BC (1998) Clusters of resistance genes in plants evolve by divergent selection and a birth-and-death process. Genome Res 8:1113-1130. 10.1101/gr.8.11.1113
53. Moore JW, Herrera-Foessel S, Lan C et al (2015) A recently evolved hexose transporter variant confers resistance to multiple pathogens in wheat. Nat Genet 47:1494-1498. https://doi.org/10.1038/ng.3439
54. Narusaka Y, Narusaka M, Park P et al (2004) RCH1 a locus in Arabidopsis that confers resistance to the hemibiotrophic fungal pathogen *Colletotrichum higginsianum*. Mol Plant Microbe Interact 17:749-762. https://doi.org/10.1094/MPMI.2004.17.7.749
55. Nene YL (1988) Multiple-disease resistance in grain legumes. Annu Rev Phytopathol 26:203-217. https://doi.org/10.1146/annurev.py.26.090188.001223
56. Paudel B, Zhuang Y, Galla A, Dahal S, Qiu Y, Ma A, Raihan T, Yen Y (2020) WFhb1-1 plays an important role in resistance against Fusarium head blight in wheat. Sci Rep 10:1-15. https://doi.org/10.1038/s41598-020-64777-9

57. Perochon A, Kahla A, Vranić M, Jia J, Malla KB, Craze M, Wallington E, Doohan FM (2019) A wheat NAC interacts with an orphan protein and enhances resistance to Fusarium head blight disease. Plant Biotechnol J 17:1892-1904. https://doi.org/10.1111/pbi.13105
58. Pfeifer M, Kugler KG, Sandve SR, Zhan B, Rudi H, Hvidsten TR, Mayer KF, Olsen OA, International Wheat Genome Sequencing Consortium (2014) Genome interplay in the grain transcriptome of hexaploid bread wheat. Science 345:6194 10.1126/science.1250091
59. Pooja S, Sharma RB, Singh AK, Rakesh S, Sundeep K (2014) Multiple disease resistance in wheat: need of today. Wheat Information Service 118:7-16.
60. Ramírez-González RH, Borrill P, Lang D et al (2018) The transcriptional landscape of polyploid wheat. Science 361:6403. 10.1126/science.aar6089
61. Rana M, Kaldate R, Nabi SU, Wani SH, Khan H (2021) Marker-Assisted Breeding for Resistance Against Wheat Rusts. In Physiological Molecular and Genetic Perspectives of Wheat Improvement (pp 229-262) Springer Cham https://doi.org/10.1007/978-3-030-59577-7_11
62. Schnippenkoetter W, Lo C, Liu G et al (2017) The wheat Lr34 multipathogen resistance gene confers resistance to anthracnose and rust in sorghum. Plant Biotechnol J 15:1387-1396. https://doi.org/10.1111/pbi.12723
63. Schweiger W, Steiner B, Vautrin S et al (2016) Suppressed recombination and unique candidate genes in the divergent haplotype encoding Fhb1 a major Fusarium head blight resistance locus in wheat. Theor Appl Genet 129:1607-1623. https://doi.org/10.1007/s00122-016-2727-x
64. Schweizer P, Stein N (2011) Large-scale data integration reveals colocalization of gene functional groups with meta-QTL for multiple disease resistance in barley. Mol Plant Microbe Interact 24:1492-1501. https://doi.org/10.1094/MPMI-05-11-0107
65. Sharma A, Srivastava P, Mavi GS, Kaur S, Kaur J, Bala R, Sohu VS, Chhuneja P, Bains NS (2021) Resurrection of wheat cultivar 'PBW343'using marker assisted gene pyramiding for rust resistance. Front Plant Sci 12:42. https://doi.org/10.3389/fpls.2021.570408
66. Simón MR, Ayala FM, Cordo CA, Röder MS, Börner A (2004) Molecular mapping of quantitative trait loci determining resistance to septoria tritici blotch caused by *Mycosphaerella graminicola* in wheat. Euphytica 138:41-48. https://doi.org/10.1023/B:EUPH.0000047059.57839.98
67. Singh K, Batra R, Sharma S et al (2021) WheatQTLdb: a QTL database for wheat. Mol Genet Genom 1-6 https://doi.org/10.1007/s00438-021-01796-9
68. Somers DJ, Isaac P, Edwards K (2004) A high-density microsatellite consensus map for bread wheat (*Triticum aestivum* L). Theor Appl Genet 109:1105-1114.
69. Soriano JM, Royo C (2015) Dissecting the genetic architecture of leaf rust resistance in wheat by QTL meta-analysis. Phytopathology 105:1585-1593. https://doi.org/10.1094/PHYTO-05-15-0130-R
70. Sosnowski O, Charcosset A, Joets J (2012) BioMercator V3: an upgrade of genetic map compilation and quantitative trait loci meta-analysis algorithms. Bioinformatics 28:2082-2083. https://doi.org/10.1093/bioinformatics/bts313

71. Takahashi H, Miller J, Nozaki Y (2002) RCY1 an *Arabidopsis thaliana* RPP8/HRT family resistance gene conferring resistance to cucumber mosaic virus requires salicylic acid ethylene and a novel signal transduction mechanism. Plant J 32:655-667. https://doi.org/10.1046/j.1365-313X.2002.01453.x
72. Venske E, Dos Santos RS, Farias DDR, Rother V, da Maia LC, Pegoraro C, Costa de Oliveira A (2019) Meta-analysis of the QTLome of Fusarium head blight resistance in bread wheat: refining the current puzzle. Frontiers Plant Sci 10:727. https://doi.org/10.3389/fpls.2019.00727
73. Veyrieras JB, Goffinet B, Charcosset A (2007) MetaQTL: a package of new computational methods for the meta-analysis of QTL mapping experiments. BMC Bioinformatics 8:1-16. https://doi.org/10.1186/1471-2105-8-49
74. Wang S, Wong D, Forrest K et al (2014) Characterization of polyploid wheat genomic diversity using a high-density 90 000 single nucleotide polymorphism array. Plant Biotechnol J 12:787-796. https://doi.org/10.1111/pbi.12183
75. Wiesner-Hanks T, Nelson R (2016) Multiple disease resistance in plants. Annu Rev Phytopathol 54:229-252. https://doi.org/10.1146/annurev-phyto-080615-100037
76. Wisser RJ, Sun Q, Hulbert SH, Kresovich S, Nelson RJ (2005) Identification and characterization of regions of the rice genome associated with broad-spectrum quantitative disease resistance Genetics 169:2277-2293. https://doi.org/10.1534/genetics.104.036327
77. Xing L, Gao L, Chen Q, Pei H, Di Z, Xiao J, Wang H, Ma L, Chen P, Cao A, Wang X (2018) Over-expressing a UDP-glucosyltransferase gene (*Ta-UGT 3*) enhances Fusarium Head Blight resistance of wheat. Plant Growth Regulation 84:561-571. https://doi.org/10.1007/s10725-017-0361-5
78. Yang F, Li W, Jørgensen HJ (2013) Transcriptional reprogramming of wheat and the hemibiotrophic pathogen Septoria tritici during two phases of the compatible interaction . PLoS One 8:pe81606. https://doi.org/10.1371/journal.pone.0081606
79. Yang Y, Amo A, Wei D, Chai Y, Zheng J, Qiao P, Cui C, Lu S, Chen L, Hu YG (2021) Large-scale integration of meta-QTL and genome-wide association study discovers the genomic regions and candidate genes for yield and yield-related traits in bread wheat. Theor Appl Genet 1-27. https://doi.org/10.1007/s00122-021-03881-4
80. Zheng T, Hua C, Li L, Sun Z, Yuan M, Bai G, Humphreys G, Li T (2020) Integration of meta-QTL discovery with omics: Towards a Mol Breed platform for improving wheat resistance to Fusarium head blight. Crop J https://doi.org/10.1016/j.cj.2020.10.006
81. Zwart RS, Thompson JP, Milgate AW, Bansal UK, Williamson PM, Raman H, Bariana HS (2010) QTL mapping of multiple foliar disease and root-lesion nematode resistances in wheat. Mol Breed 26:107-124. https://doi.org/10.1007/s11032-009-9381-9

Figures

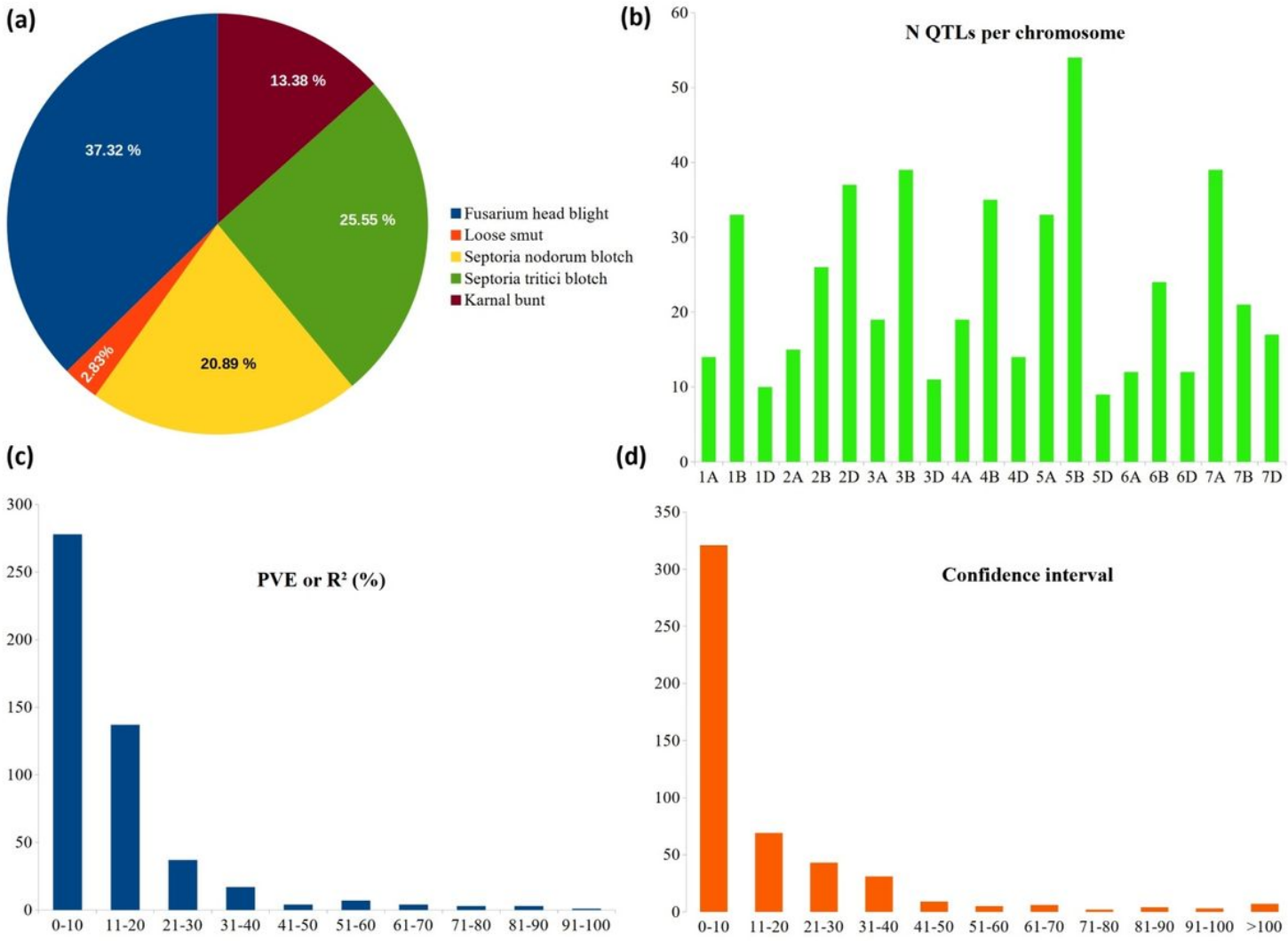

Figure 1

Salient features of the QTLs: (a) distribution of QTLs associated with different diseases, (b) number of QTLs per chromosome, (c) PVE and (d) CI of the collected QTLs.

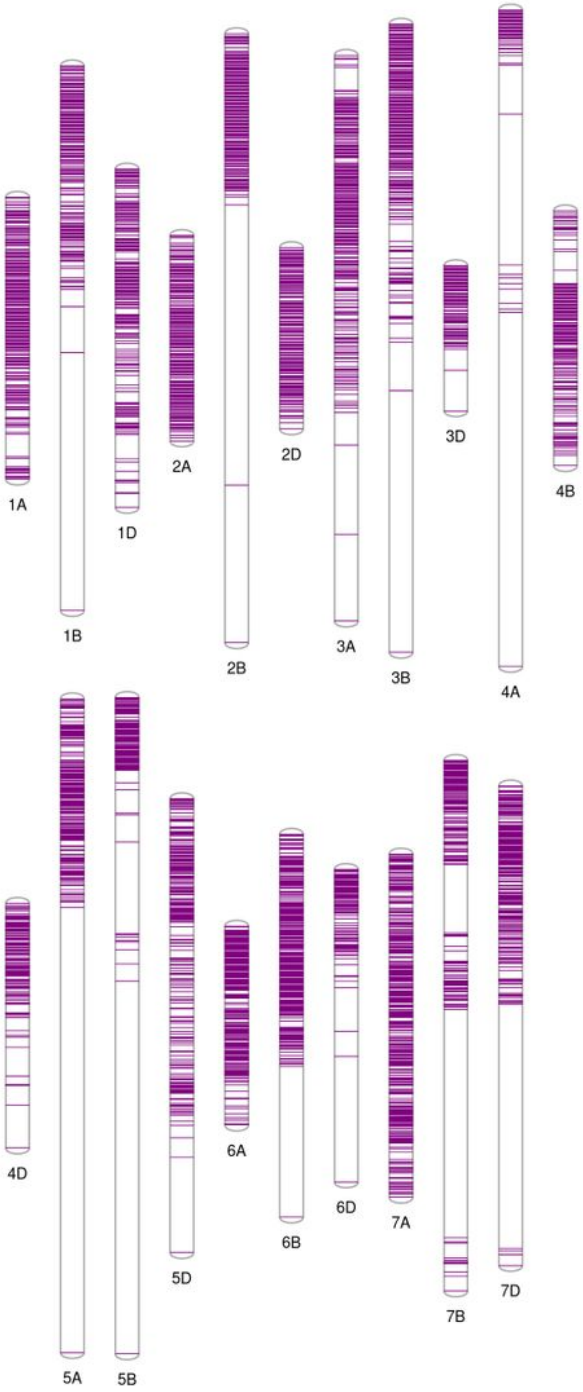

Figure 2

Markers density on different wheat chromosomes.

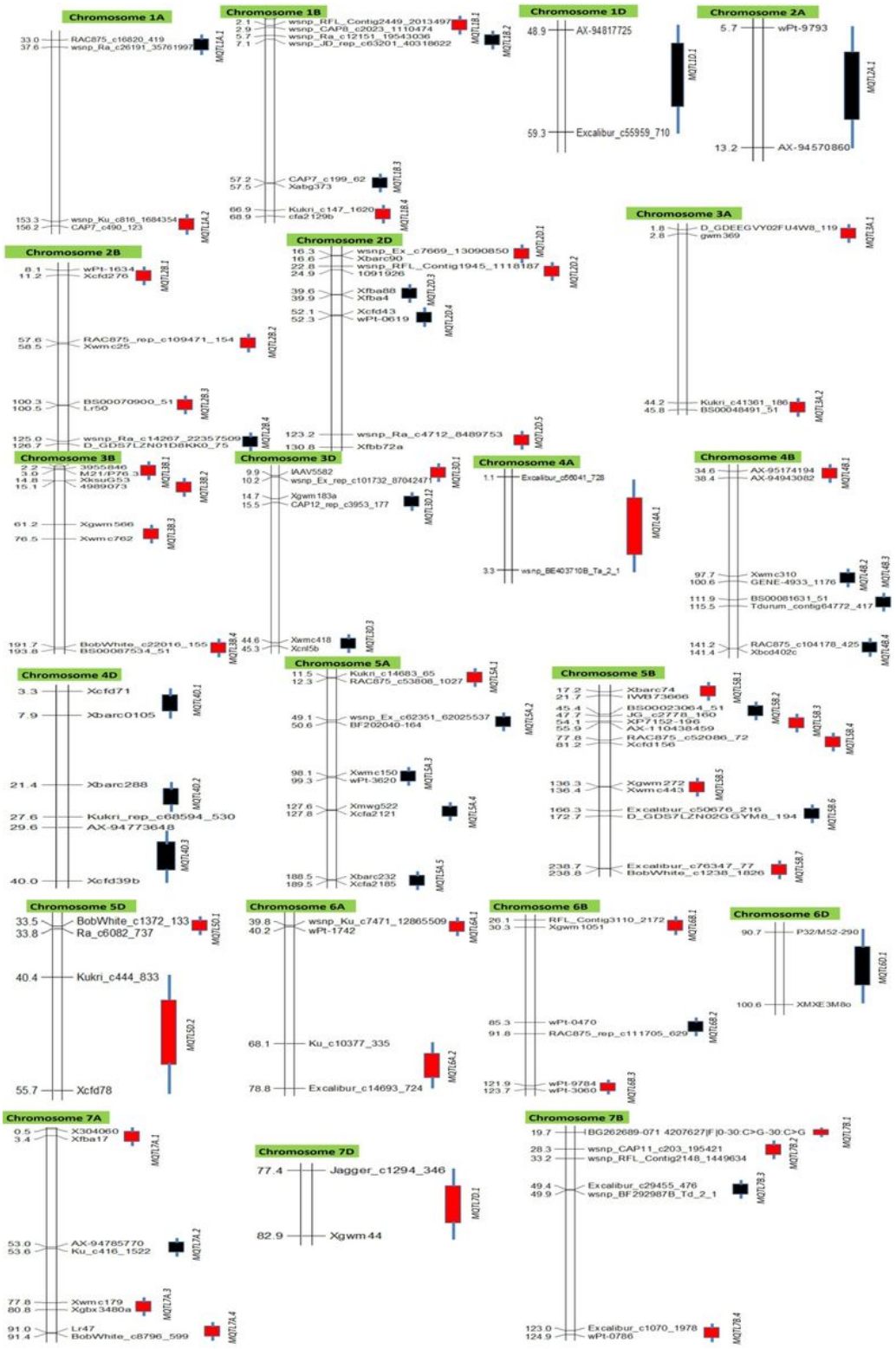

Figure 3

Distribution of 63 MQTLs on 21 wheat chromosomes. The boxes on the right of each chromosomes represent the position of MQTLs (red boxes represent the positions of GWAS-validated MQTLs). Only the flanking markers of the MQTLs have been shown in the figure for better visualization.

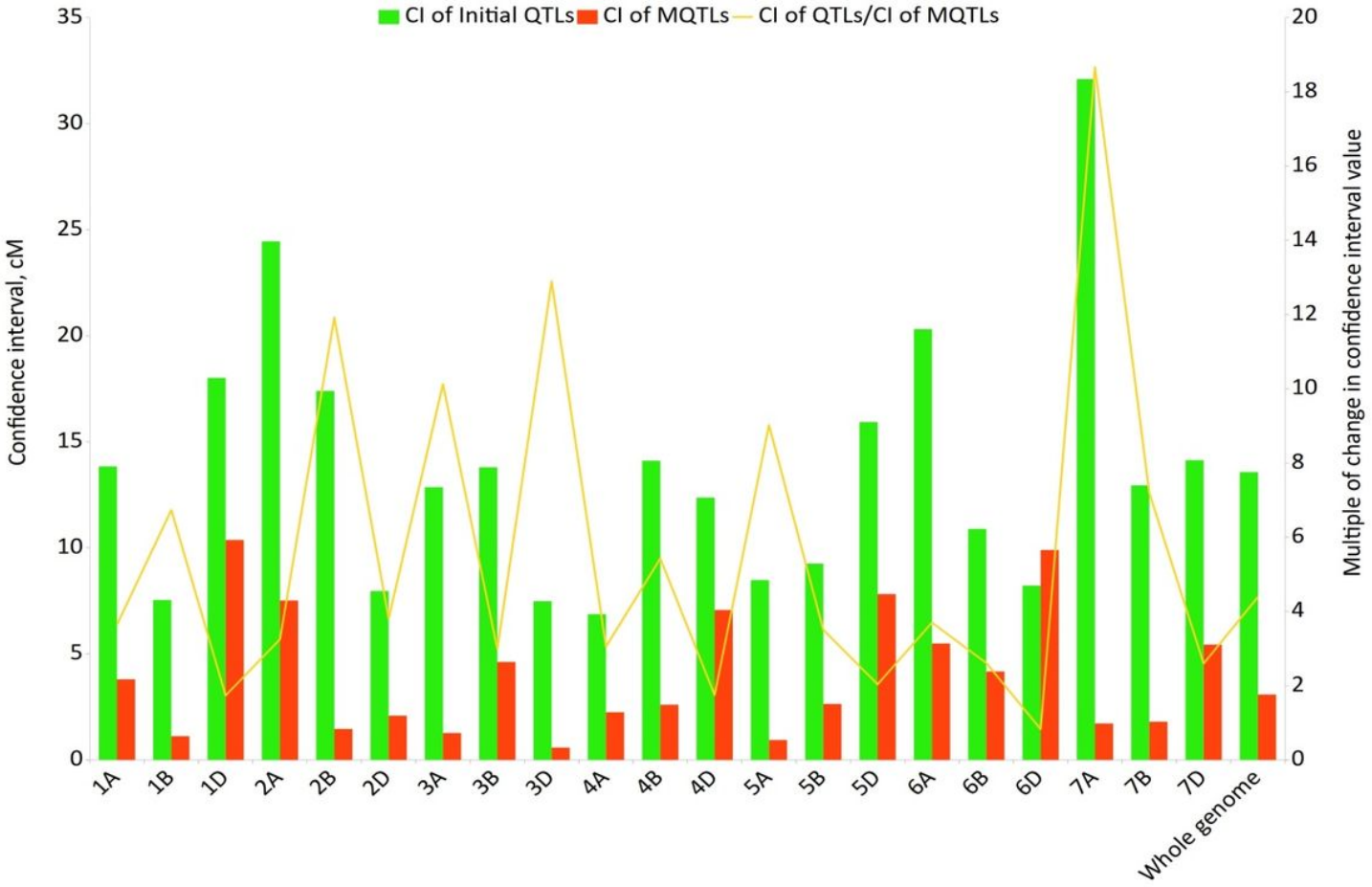

Figure 4

The reduction degree of CI of QTLs after meta-QTL analysis.

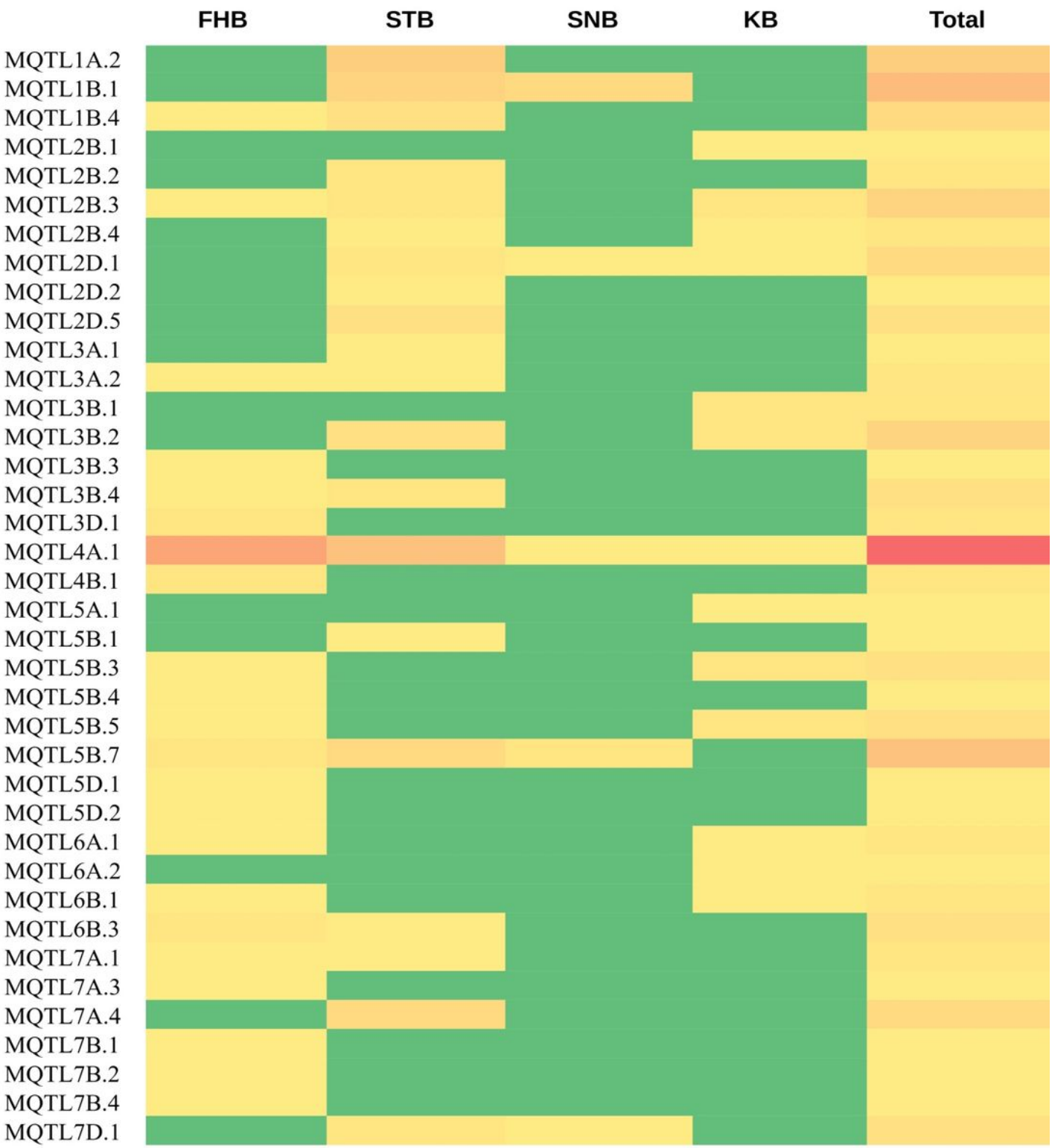

Figure 5

The co-localization of MQTLs with MTAs (derived from GWAS) associated with different diseases. The changes in colour from green to red represents the frequency of MTAs co-localized with MQTLs (from 0 to 23).

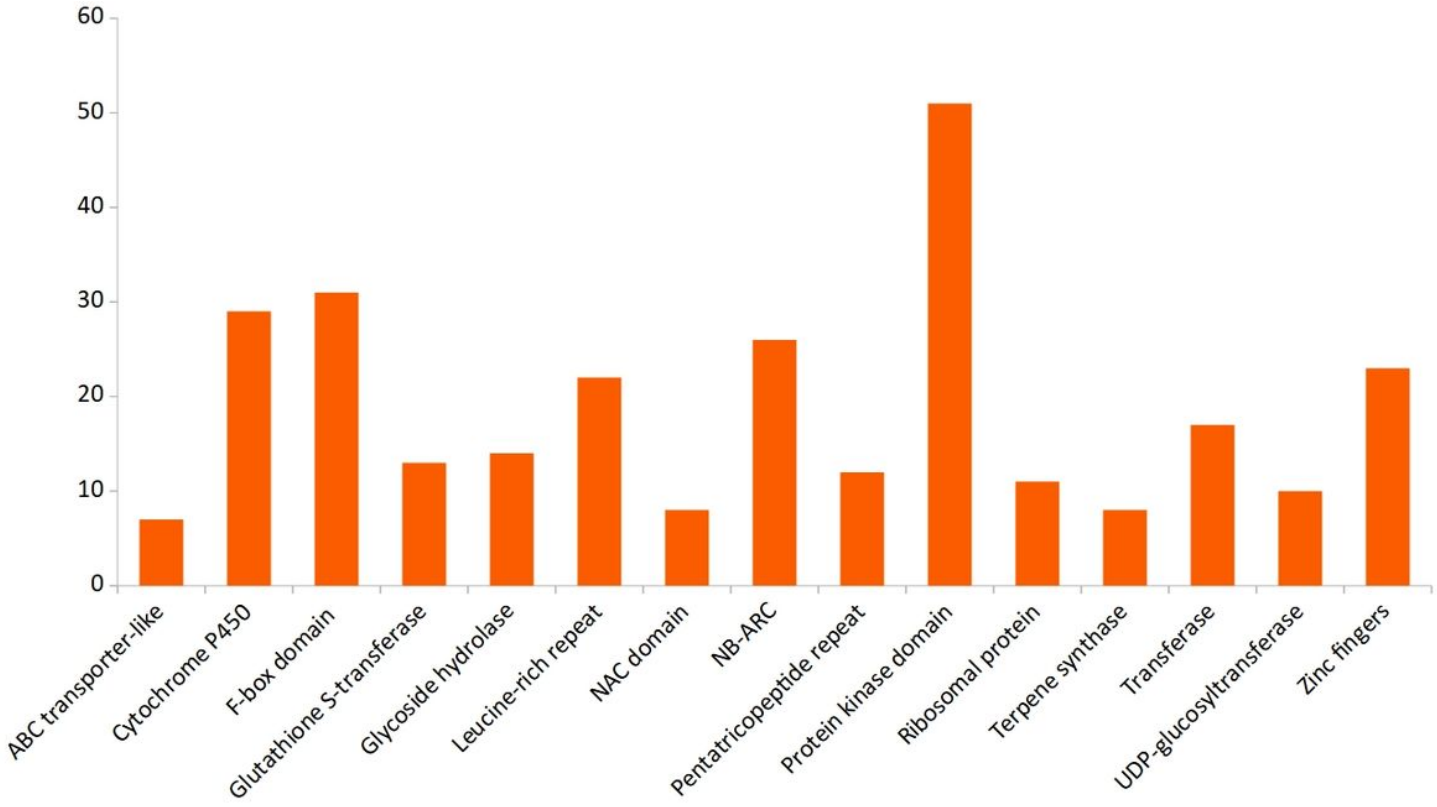

Figure 6

Histogram showing frequencies of CGs encoding proteins involved in disease resistance.

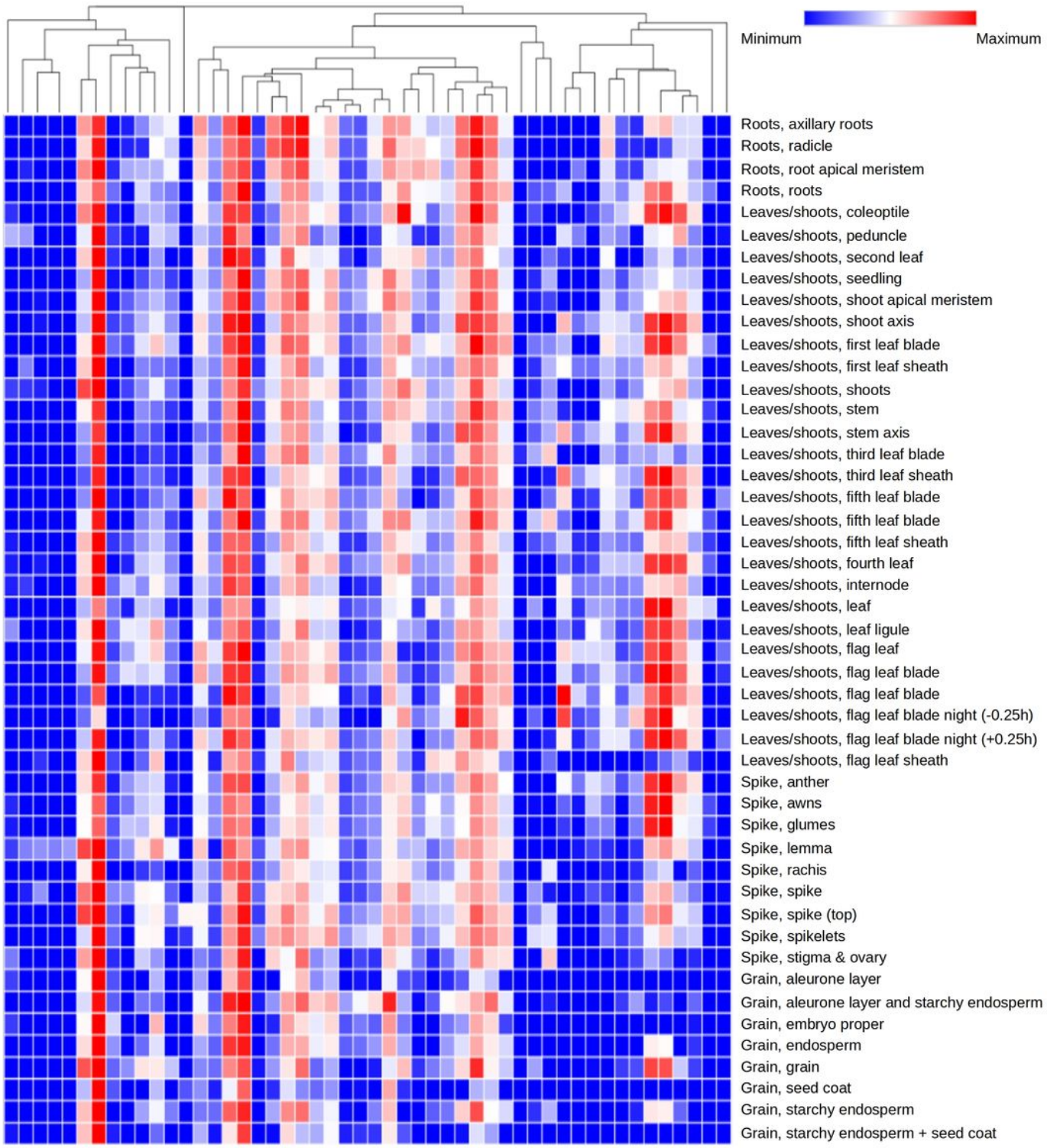

Figure 7

Expression pattern of 50 CGs (deferentially expressed under different pathogen inoculations) in 47 tissues. All transcriptome data was downloaded from expVIP. The changes in color from blue to red signifies alteration in level of expression from low to high.